

CERN-TH/97-219
 IFUM 589/FT
 hep-ph/9709360

NEXT-TO-LEADING-ORDER CORRECTIONS TO
 THE PRODUCTION OF HEAVY-FLAVOUR
 JETS IN e^+e^- COLLISIONS

Paolo NASON¹,
 CERN, TH Division, Geneva, Switzerland

Carlo OLEARI
 Dipartimento di Fisica, Università di Milano and INFN, Milan, Italy

Abstract

In this paper we describe the calculation of the process $e^+e^- \rightarrow Z/\gamma \rightarrow Q\bar{Q} + X$, where Q is a heavy quark, at order α_s^2 .

CERN-TH/97-219
 July 1, 2021

¹On leave of absence from INFN, Milan, Italy

1 Introduction

Radiative corrections to jet production in e^+e^- annihilation were computed a long time ago [1, 2, 3]. These calculations were, however, performed for massless quarks. In most practical applications this is sufficient, since, at relatively low energy, the b fraction is strongly suppressed, and at high energy (i.e. on the Z peak and beyond) mass effects are suppressed. Nevertheless there are several reasons why a next-to-leading-order calculation is desirable. First of all, at sufficiently high energies, top pairs will be produced and mass effects there are very likely to be important. A second reason is to understand the relevance of mass corrections, due to bottom production, to the determination of α_s from event shape variables. As a third point, quantities such as the heavy-flavour momentum correlation [4, 5], although well defined in the massless limit, cannot be computed using the massless results of refs. [1, 2, 3].

In this paper we describe a recently completed next-to-leading-order calculation of the heavy-flavour production cross section in e^+e^- collisions, including quark mass effects. Very recently, two calculations have appeared in the literature that address the same problem [6, 7, 8]. They both use a slicing method in order to deal with infrared divergences. In our work, we preferred to use a subtraction method, since, in this way, we do not need to worry about taking the limit for small cutoff parameters². We were able to perform a partial comparison of our result with that of ref. [6], and found satisfactory agreement. In the older work of ref. [10], a calculation of the process $e^+e^- \rightarrow Q\bar{Q}gg$ has been given, but virtual corrections to the process $e^+e^- \rightarrow Q\bar{Q}g$ were not included. In ref. [11], the NLO corrections to the production of a heavy quark pair plus a photon are given, including both real and virtual contributions.

The paper is organized as follows. In Section 2 we give a brief outline of the calculation. In Section 3 we introduce our kinematical definitions and conventions. In Section 4 we present a somewhat detailed description of the calculation. In Section 5 we describe a few checks on our result. Finally, Section 6 contains some concluding remarks.

²Subtraction methods for the calculation of radiative corrections to $e^+e^- \rightarrow \text{jets}$ have been used in refs. [1, 9], and they have also been successfully employed in the calculation of hadronic production processes.

2 Generalities

We begin by showing in Fig. 1 the Feynman diagrams for a Born term (a), a virtual correction term (b) and two real next-to-leading contributions (c,d). Next-to-leading

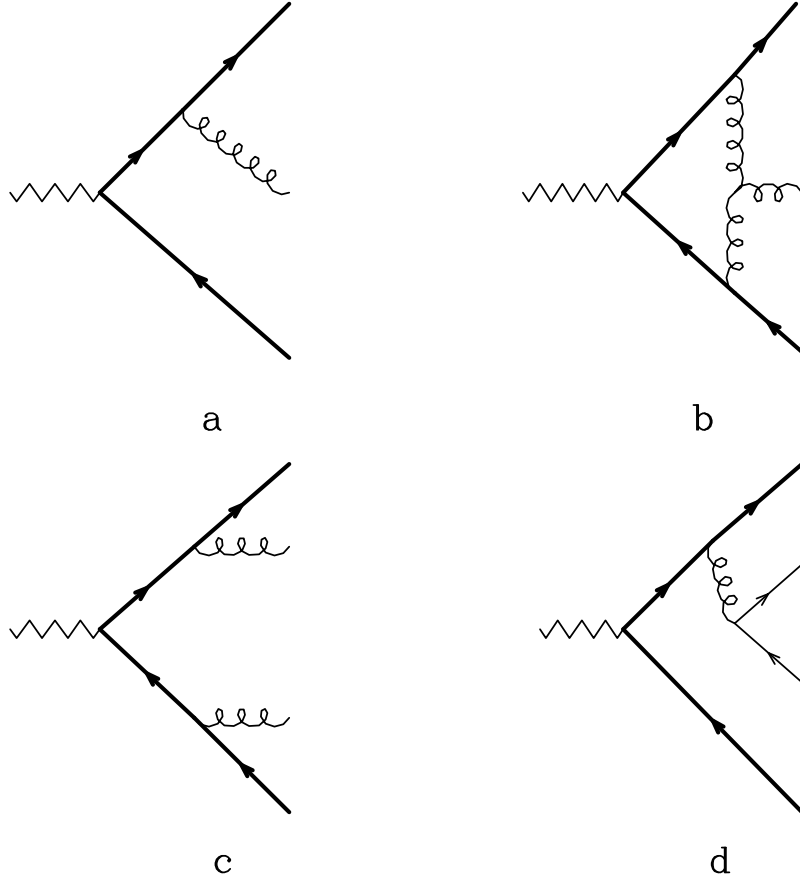


Figure 1: *Some of the diagrams contributing to the process $Z/\gamma \rightarrow Q\bar{Q} + X$: a Born graph (a), a virtual graph (b), a real emission graph (c) and a real emission graph with light quarks in the final state (d).*

corrections arise from the interference of the virtual graphs with the Born graphs, and from the square of the real graphs. Observe that we always deal with the cross section for the production of the heavy quark pair plus the emission of at least one extra particle (i.e. a gluon or a quark). The inclusion of virtual graphs with only a $Q\bar{Q}$ pair in the final state is not needed if one computes three-jet-related quantities. Furthermore, since we deal with unoriented shape variables, the kinematics of these virtual graphs is fully specified, and in order to account for them it is enough to

include, in the final result, a two-body contribution normalized in such a way that one obtains the correct total heavy-flavour cross section at order α_s^2 (see [12] and references therein).

Virtual graphs, besides the usual ultraviolet divergences (which are removed by renormalization), also have infrared and collinear divergences. These cancel when suitable infrared-safe final-state variables are considered. Our treatment of the infrared cancellation is such that the final result is expressed as a partonic event generator, in which pairs of weighted correlated events are produced. Shape variables are computed independently for each generated event, and histogrammed with the corresponding weight. Infrared-safe shape variables give rise to finite distributions. No arbitrary cutoff is needed in this calculation in order to implement the cancellation of virtual and real infrared divergences, since this cancellation takes place between the two correlated events. Therefore, one does not have to worry about taking the limit for a vanishing soft cutoff. This method is similar to the one of ref. [9], which was used there to compute a large class of shape variable distributions for the LEP experiments.

At next-to-leading order, several complications arise that must be considered. In fact, heavy flavours may also be produced by a gluon splitting mechanism, and diagrams with four heavy quarks in the final state are also present. Interferences between gluon splitting and direct production should also be considered. It is useful, however, to separate the various contributions in the following way. We examine each contribution in terms of cut Feynman graphs, which represent, individually, a single contribution to the cross section. We classify the cut graphs according to the following types:

- A) Contributions where the electroweak currents in the cut graphs are coupled to the same heavy-flavour loop, and there is a single $Q\bar{Q}$ pair in the final state. These contributions are the most complex from the point of view of renormalization and soft and collinear divergences. They constitute the hard part of the calculation. They include graphs in which a pair of gluons or a pair of light quarks is present in the final state. We will call them A-type. We show some of them in Fig. 2.
- B) Contributions where there are two $Q\bar{Q}$ pairs in the final state. These include cut graphs with a single heavy-flavour loop coupled to the weak currents, graphs with two heavy-flavour loops, one of which is coupled to the weak currents, and

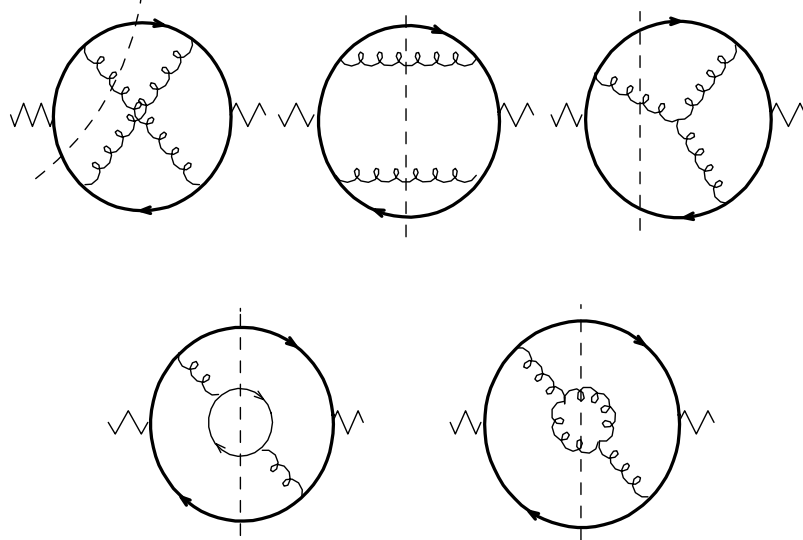


Figure 2: *Some of the diagrams of A-type. Depending upon the cut, each graph represents a contribution coming from the square of the four-particle final state or from the interference between the tree-level graph with a virtual correction.*

graphs with two heavy-flavour loops, where each loop is coupled to one weak current. These contributions are finite, and their computation is a straightforward algebraic problem. We will call them B-type. We have collected some of them in Fig. 3.

- C) Contributions where the electroweak currents are coupled to light quarks. Also these contributions are finite, and easy to compute. The heavy-flavour pair in the final state is generated by gluon splitting. We will call them C-type.
- D) Interference between terms in which the weak current is coupled to the heavy quarks and to quarks of different flavours. These terms have the structure of Fig. 4. By Furry’s theorem, they must vanish for vector currents. For axial currents, they cancel in pairs of up-type and down-type quarks, because they have opposite axial coupling. Thus, the up-quark contribution cancels with the down quark, and, if the charm mass is neglected, the charm contribution cancels with the strange. Only the graph with a top quark loop remains. We call these graphs D-type.
- E) Graphs with two heavy-flavour loop coupled to the weak current, one of which

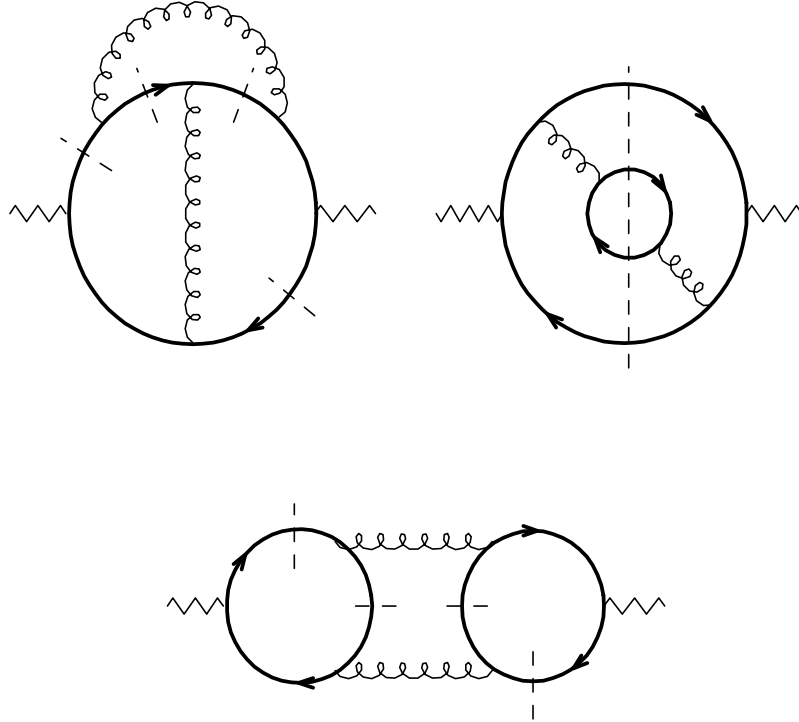


Figure 3: *Some of the diagrams of B-type.*

is virtual. We call these graphs E-type. They pair naturally with the D-type graphs with the top loop, since in cases of practical interest the top loop is also virtual.

Most of the following discussion will deal with A-type graphs, since the other cases are either straightforward, or they have already been considered in the literature. For example, graphs of B and C type have been computed in ref. [10], and graphs of type D and E have been considered in ref. [13]. There is, however, one extra contribution that should be considered together with the A-type graphs, that is to say, virtual graphs in which a heavy-flavour loop corrects the gluon propagator. These graphs are ultraviolet divergent, and so their inclusion is mandatory if one wants to have the complete cancellation of ultraviolet divergences after renormalization. We will discuss this contribution in detail when we deal with renormalization.

A-type graphs contain ultraviolet, soft and collinear divergences that must be regulated. Soft divergences arise when, in addition to the basic $Q\bar{Q}g$ final state, an extra soft gluon is emitted, giving rise to a real soft divergent contribution. Collinear

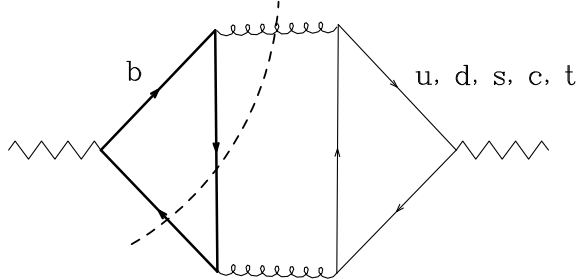


Figure 4: *Structure of cut graphs of D-type.*

singularities arise when the final-state gluon in the $Q\bar{Q}g$ process undergoes a real (virtual) splitting into either a gg pair or a $q\bar{q}$ pair. In the first case, the collinear gluon can also be soft, so that collinear singularities can overlap with soft singularities.

In order to regularize all singularities we used dimensional regularization. At first sight, this procedure would seem in conflict with the presence of the axial coupling. In fact, for the class of graphs of A-type, there is a simple trick to avoid this problem. First of all, we notice that for unoriented shape variables the axial-vector interference cannot contribute. In fact, for the three-parton final state there are not enough momentum vectors to construct an invariant with an ϵ symbol. For the four-parton final state one could in principle build such an invariant, but the cross section must be symmetric in the light parton momenta, so that such an invariant cannot survive. We then consider the case of a generic vector current coupled to two fermions with different masses m_1 and m_2 . One can then easily convince oneself that the case of the axial coupling can be obtained by setting $m_1 = m$ and $m_2 = -m$, since one can turn $-m$ into m by a chiral rotation. This procedure is bound to work if there are no anomalies involved in the calculation, and this is certainly the case for our A-type graphs. We will therefore proceed to compute the $\mathcal{O}(\alpha_s^2)$ three- and four-body contributions in $d = 4 - 2\epsilon$ dimensions. We will get a result of the form

$$d\sigma = \left(\frac{\alpha_s}{2\pi}\right) d\sigma^{(1)} + \left(\frac{\alpha_s}{2\pi}\right)^2 d\sigma^{(2)} \quad (2.1)$$

$$d\sigma^{(2)} = \frac{d\sigma_3^{(2)}}{d\Phi_3} d\Phi_3 + \frac{d\sigma_4^{(2)}}{d\Phi_4} d\Phi_4 \quad (2.2)$$

where the suffix 3 and 4 refers to the three- and four-body contributions. The ultra-violet, collinear and soft singularities will manifest themselves as single and double poles in $1/\epsilon$ in the three-body contribution, and as singularities arising from the

phase-space integration in the four-body contribution. We will call q the total incoming invariant momentum and p, p' the momenta of the outgoing heavy quark and antiquark. Furthermore, we introduce the variables

$$x_1 = \frac{2q \cdot p}{q^2}, \quad x_2 = \frac{2q \cdot p'}{q^2}, \quad y = \frac{(q - p - p')^2}{q^2}. \quad (2.3)$$

Here y characterizes the mass of the light system accompanying the heavy-quark pair. Thus, for Born and virtual graphs we will always have $y = 0$.

In addition

$$\begin{aligned} d\Phi_3 &= dx_1 dx_2 J_3(x_1, x_2) \\ d\Phi_4 &= dx_1 dx_2 dy d^2Y J_4(x_1, x_2, y, Y), \end{aligned} \quad (2.4)$$

where Y represents the other two variables that are necessary to describe the four-body final state. In order to implement the cancellation of the soft and collinear singularities, we now imagine to compute some physical quantity G , function of the final-state variables. The reader may think of G as the combination of theta functions that characterize a histogram bin for some infrared-safe shape variable. In general the definition of G will be specified for any number of particles in the final state. Since we are only dealing with three- and four-parton final states, as far as we are concerned here, G is characterized by only two functions, $G^{(3)}(x_1, x_2)$ and $G^{(4)}(x_1, x_2, y, Y)$. Soft and collinear finiteness of G will require that

$$\lim_{y \rightarrow 0} G^{(4)}(x_1, x_2, y, Y) = G^{(3)}(x_1, x_2). \quad (2.5)$$

We will have

$$\begin{aligned} \int d\sigma^{(2)} G &= \int dx_1 dx_2 J_3(x_1, x_2) \frac{d\sigma_3^{(2)}}{d\Phi_3} G^{(3)}(x_1, x_2) \\ &+ \int dx_1 dx_2 dy d^2Y J_4(x_1, x_2, y, Y) \frac{d\sigma_4^{(2)}}{d\Phi_4} G^{(4)}(x_1, x_2, y, Y), \end{aligned} \quad (2.6)$$

where each term on the right-hand side contains soft and collinear divergences that cancel in the sum. This formula will be rewritten in the following way:

$$\begin{aligned} \int d\sigma^{(2)} G &= \int dx_1 dx_2 G^{(3)}(x_1, x_2) \left\{ \frac{d\sigma_3^{(2)}}{d\Phi_3} J_3(x_1, x_2) + \int dy d^2Y \frac{d\bar{\sigma}_4^{(2)}}{d\Phi_4} J_4(x_1, x_2, y, Y) \right\} \\ &+ \int dx_1 dx_2 dy d^2Y J_4(x_1, x_2, y, Y) \left\{ \frac{d\sigma_4^{(2)}}{d\Phi_4} G^{(4)}(x_1, x_2, y, Y) - \frac{d\bar{\sigma}_4^{(2)}}{d\Phi_4} G^{(3)}(x_1, x_2) \right\} \end{aligned} \quad (2.7)$$

where $\bar{\sigma}_4^{(2)}$ is chosen in such a way that it has the same soft and collinear singular part as $\sigma_4^{(2)}$, or, schematically

$$\lim_{y \rightarrow 0} \frac{\frac{d\bar{\sigma}_4^{(2)}}{d\Phi_4}}{\frac{d\sigma_4^{(2)}}{d\Phi_4}} = 1. \quad (2.8)$$

The first term of eq. (2.7) can be computed analitically. The $1/\epsilon$ single and double poles present in $d\sigma_3^{(2)}/d\Phi_3$ all cancel with the poles arising from the $dy d^2Y$ integration of $d\bar{\sigma}_4^{(2)}/d\Phi_4$, and thus this term is finite.

The second term in eq. (2.7), because of eqs. (2.5) and (2.8), has no soft and collinear singularities, and thus can be evaluated directly in four dimensions³. It is easy to see how the computation of this term can be implemented numerically. Assuming for simplicity that we can generate four-body configurations uniformly in the four-body phase space, to each four-body configuration x_1, x_2, y, Y we associate two events: one four-body event with kinematics x_1, x_2, y, Y and weight $d\sigma_4^{(2)}/d\Phi_4$, and one three-body event with kinematics x_1, x_2 (and $y = 0$), and weight $-d\bar{\sigma}_4^{(2)}/d\Phi_4$. The computation of a shape variable using the above scheme reproduces exactly the second term of eq. (2.7).

3 Kinematics

3.1 Three-body kinematics

We consider the following three-body process

$$e^+ (p'_e) + e^- (p_e) \rightarrow Z/\gamma (q) \rightarrow Q(p) + \bar{Q}(p') + g(k) \quad (3.1)$$

where Q is the massive quark, and the momenta of the particles satisfy

$$p^2 = p'^2 = m^2 \quad k^2 = 0.$$

Since we are interested in unoriented shape variables, we can express the three-body phase space in terms of two variables, which we choose to be

$$x_1 = \frac{2q \cdot p}{q^2}, \quad x_2 = \frac{2q \cdot p'}{q^2}. \quad (3.2)$$

³ Observe that both eq. (2.5) and eq. (2.8) must be satisfied in d dimensions in order for this argument to apply.

Defining in addition

$$\rho = \frac{4m^2}{q^2}, \quad (3.3)$$

the three-body phase space in $d = 4 - 2\epsilon$ dimensions takes the form

$$\begin{aligned} (\text{PS})^{(3)} = & H \int_{\sqrt{\rho}}^1 dx_1 \int_{x_{2-}}^{x_{2+}} dx_2 \\ & \left\{ 4(x_1^2 - \rho)(x_2^2 - \rho) - [x_g^2 - (x_1^2 - \rho) - (x_2^2 - \rho)]^2 \right\}^{-\epsilon} \end{aligned} \quad (3.4)$$

where:

$$H = \frac{1}{\Gamma(2 - 2\epsilon)} \frac{q^2}{2(4\pi)^3} \left(\frac{16\pi}{q^2} \right)^{2\epsilon} \quad (3.5)$$

$$x_{2\pm} = \frac{1}{4(1 - x_1) + \rho} \left[2(1 - x_1)(2 - x_1) + \rho(2 - x_1) \pm 2(1 - x_1) \sqrt{x_1^2 - \rho} \right]. \quad (3.6)$$

3.2 Four-body kinematics

The four-body processes we are considering are

$$\begin{aligned} e^+(p'_e) + e^-(p_e) &\rightarrow Z/\gamma(q) \rightarrow Q(p) + \bar{Q}(p') + g(k) + g(l) \\ e^+(p'_e) + e^-(p_e) &\rightarrow Z/\gamma(q) \rightarrow Q(p) + \bar{Q}(p') + q(k) + \bar{q}(l), \end{aligned}$$

where q is the massless quark. The momenta satisfy

$$l^2 = k^2 = 0 \quad p^2 = p'^2 = m^2. \quad (3.7)$$

In the centre-of-mass system of the two massless particles, we have

$$\begin{aligned} l &= l_0(1, \dots, \sin\theta\sin\phi, \sin\theta\cos\phi, \cos\theta) \\ k &= k_0(1, \dots, -\sin\theta\sin\phi, -\sin\theta\cos\phi, -\cos\theta) \\ p &= p_0 \left(1, \dots, 0, 0, \sqrt{1 - \frac{m^2}{p_0^2}} \right) \\ p' &= p'_0 \left(1, \dots, 0, \sqrt{1 - \frac{m^2}{p'_0^2}} \sin\alpha, \sqrt{1 - \frac{m^2}{p'_0^2}} \cos\alpha \right) \end{aligned}$$

where the dots indicate $d - 3$ equal and opposite components in the expression for l and k , and $d - 3$ zeros in the expression for p and p' .

To describe the unoriented four-body phase space, we need five independent variables, which we choose to be

$$x_1 = \frac{2q \cdot p}{q^2}, \quad x_2 = \frac{2q \cdot p'}{q^2}, \quad y = \frac{(k+l)^2}{q^2}, \quad \theta, \quad \phi. \quad (3.8)$$

We thus have

$$l_0 = k_0 = \sqrt{q^2} \frac{\sqrt{y}}{2}, \quad p_0 = \sqrt{q^2} \frac{1 - x_2 - y}{2\sqrt{y}}, \quad p'_0 = \sqrt{q^2} \frac{1 - x_1 - y}{2\sqrt{y}} \quad (3.9)$$

and

$$\cos \alpha = \frac{y(\rho - x_1 - x_2) + (1 - x_1)(1 - x_2) - y^2}{\sqrt{(1 - x_1 - y)^2 - 4\rho y} \sqrt{(1 - x_2 - y)^2 - 4\rho y}}. \quad (3.10)$$

Setting

$$v = \frac{1}{2}(1 - \cos \theta)$$

and defining

$$x_g = 2 - x_1 - x_2 \quad (3.11)$$

$$\begin{aligned} y_{\pm} &= \frac{1}{4} \left[\pm 2\sqrt{x_1^2 - \rho} \sqrt{x_2^2 - \rho} + x_g^2 - (x_1^2 - \rho) - (x_2^2 - \rho) \right] \\ x_{1+} &= 2 - \frac{2 - \rho}{2 - \sqrt{\rho}} \end{aligned} \quad (3.12)$$

the four-particle phase space in $d = 4 - 2\epsilon$ dimensions is

$$\begin{aligned} (\text{PS})^{(4)} &= \frac{q^2}{(4\pi)^2 \Gamma(1 - \epsilon)} \left(\frac{4\pi}{q^2} \right)^\epsilon H \\ &\times \left\{ \underbrace{\int_{\sqrt{\rho}}^1 dx_1 \int_{x_{2-}}^{x_{2+}} dx_2 \int_0^{y_+} dy}_{\text{region I}} + \underbrace{\int_{\sqrt{\rho}}^{x_{1+}} dx_1 \int_{\sqrt{\rho}}^{x_{2-}} dx_2 \int_{y_-}^{y_+} dy}_{\text{region II}} \right\} y^{-\epsilon} \\ &\times \left\{ 4(x_1^2 - \rho)(x_2^2 - \rho) - [(x_g^2 - 4y) - (x_1^2 - \rho) - (x_2^2 - \rho)]^2 \right\}^{-\epsilon} \\ &\times \int_0^1 dv [v(1 - v)]^{-\epsilon} \frac{1}{N_\phi} \int_0^\pi d\phi (\sin \phi)^{-2\epsilon} \end{aligned} \quad (3.13)$$

with

$$N_\phi = \int_0^\pi d\phi (\sin \phi)^{-2\epsilon} = 4^\epsilon \pi \frac{\Gamma(1 - 2\epsilon)}{\Gamma^2(1 - \epsilon)} \quad (3.14)$$

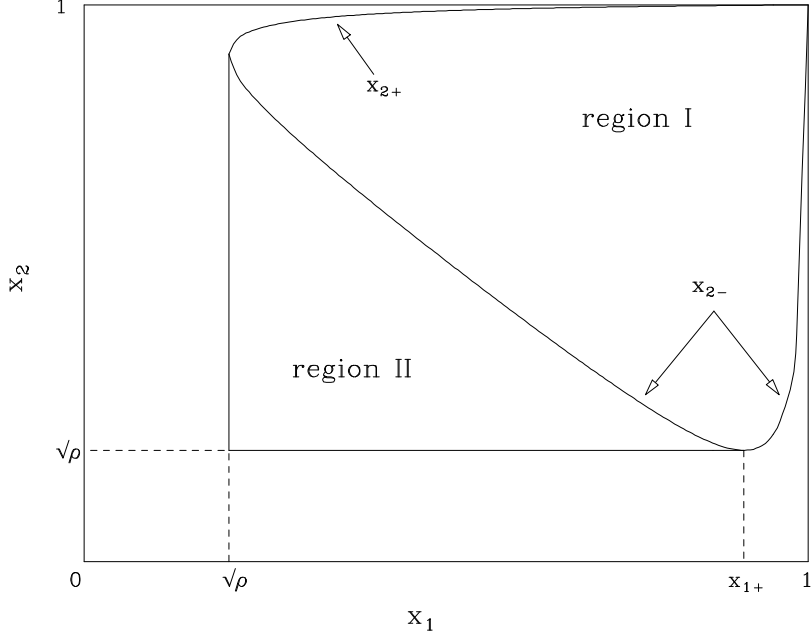


Figure 5: *The two different areas in the x_1 - x_2 plane correspond to the region I and to the region II of eq. (3.13)*

As can be seen from Fig. 5, the integration region is split into two parts, one of which (region I) is characterized by the same x_1 and x_2 integration limits as the three-body phase space. In this region, the variable y can reach 0, and therefore collinear and soft divergences arise.

Sometimes we will need an analogous set of final-state variables, in which the role of p and p' are interchanged. The variable y remains the same, x_1 and x_2 are exchanged, and the other two variables, denoted by v' and ϕ' , are related to v and ϕ by the equations

$$\begin{aligned} v' &= \frac{1}{2} \left(1 - \cos \alpha - (\sin \theta \cos \phi \sin \alpha - 2v \cos \alpha) \right) \\ \cos \phi' &= \frac{1 - \cos \alpha - 2(v - v' \cos \alpha)}{2 \sin \alpha \sqrt{v'(1 - v')}}. \end{aligned} \tag{3.15}$$

Exchanging instead the roles of l and k brings about the following transformations:

$$v \rightarrow 1 - v, \quad \phi \rightarrow \pi + \phi, \quad v' \rightarrow 1 - v', \quad \phi' \rightarrow \pi + \phi'. \tag{3.16}$$

4 Outline of the calculation

The amplitude for the process can be written (up to an irrelevant phase)

$$\begin{aligned} \bar{u}(p_e) & \left[g_Z^2 \frac{-g_{\mu\nu}}{q^2 - M_Z^2 + i\Gamma M_Z} (v_e \gamma^\mu - a_e \gamma^\mu \gamma^5) \langle 0 | J_V^\nu(0) v_Q - J_A^\nu(0) a_Q | f \rangle \right. \\ & \left. + g^2 \frac{-g_{\mu\nu}}{q^2} (c_e \gamma^\mu) \langle 0 | J_V^\nu(0) c_Q | f \rangle \right] v(p'_e), \end{aligned} \quad (4.1)$$

where f refers to states with four-momentum q . We use the notation

$$\begin{aligned} g_Z & \equiv \frac{g}{2 \sin \theta_W \cos \theta_W} \\ v_i & \equiv T_{3i} - 2c_i \sin^2 \theta_W \\ a_i & \equiv T_{3i} \end{aligned}$$

where g is the electromagnetic coupling, T_{3i} is the third component of the (left) isospin of fermion i , c_i is its electric charge in units of the positron charge and θ_W is the Weinberg angle. Since we are interested in unoriented events, and following the assumptions described in Section 2, we can neglect the axial-vector interference in the square of the amplitude. From eq. (4.1) we get the following cross section, averaged over the incoming electron beam direction

$$\begin{aligned} d\sigma & = \frac{N_c 4\pi \alpha^2}{3q^2} \left\{ dT_A \left[\rho_2(q^2) (v_e^2 + a_e^2) a_Q^2 \right] \right. \\ & \left. + dT_V \left[\rho_2(q^2) (v_e^2 + a_e^2) v_Q^2 + c_e^2 c_Q^2 - 2\rho_1(q^2) v_e v_Q c_e c_Q \right] \right\} \end{aligned}$$

where α is the electromagnetic coupling constant and $N_c = 3$ is the number of colours. In addition

$$\begin{aligned} \rho_1(q^2) & = \frac{1}{4 \sin^2 \theta_W \cos^2 \theta_W} \frac{q^2 (m_Z^2 - q^2)}{(m_Z^2 - q^2)^2 + m_Z^2 \Gamma_Z^2}, \\ \rho_2(q^2) & = \left(\frac{1}{4 \sin^2 \theta_W \cos^2 \theta_W} \right)^2 \frac{q^4}{(m_Z^2 - q^2)^2 + m_Z^2 \Gamma_Z^2}. \end{aligned}$$

We have also defined

$$\begin{aligned} dT_{V/A} & = \sum_n \mathcal{M}_{V/A}^{(f_n)} d\phi_n \\ \mathcal{M}_{V/A}^{(f_n)} & = \frac{2\pi}{N_c q^2} \left(-g_{\mu\nu} + \frac{q_\mu q_\nu}{q^2} \right) \langle 0 | J_{V/A}^\mu(0) | f_n \rangle \langle f_n | J_{V/A}^\nu(0) | 0 \rangle, \end{aligned} \quad (4.2)$$

where $d\phi_n$ represents the n -body phase space, and f_n represents an n -body final state. The $q^\mu q^\nu$ term in the projector in eq. (4.2) is, of course, irrelevant for the vector current component, but it should be kept for the axial current when the quark mass is non-zero.

In the following we will be interested in strong corrections up to the second order, and into the final states: $Q\bar{Q}$, $Q\bar{Q}g$, $Q\bar{Q}gg$ and $Q\bar{Q}q\bar{q}$. We will use the following simplified notation:

- $\mathcal{M}_{V/A}^{(2)}$ for the $Q\bar{Q}$ Born term
- $\mathcal{M}_{V/A}^{(b)}$ or \mathcal{M}_b to indicate the three-body $Q\bar{Q}g$, $\mathcal{O}(\alpha_s)$ term
- $\mathcal{M}_{V/A}^{(v)}$ or \mathcal{M}_v to indicate the three-body $Q\bar{Q}g$, $\mathcal{O}(\alpha_s^2)$ term
- $\mathcal{M}_{V/A}^{(gg)}$ or \mathcal{M}_{gg} for the four-body $Q\bar{Q}gg$, $\mathcal{O}(\alpha_s^2)$ term
- $\mathcal{M}_{V/A}^{(q\bar{q})}$ or $\mathcal{M}_{q\bar{q}}$ for the four-body $Q\bar{Q}q\bar{q}$, $\mathcal{O}(\alpha_s^2)$ term,

and equivalent ones for the $dT_{V/A}$ terms.

We will drop the V/A suffix when not referring specifically to the axial or vector contribution.

4.1 $Q\bar{Q}$ cross section

From the amplitude

$$\bar{u}(p)\Gamma_{V/A}^\mu v(p') , \quad (4.3)$$

where $\Gamma_V^\mu = \gamma^\mu$ and $\Gamma_A^\mu = \gamma^\mu\gamma^5$, we obtain the two-body cross section at zeroth order in α_s . We get

$$\mathcal{M}_V^{(2)} = \frac{2\pi}{N_c q^2} N_c 4q^2 \left(1 + \frac{\rho}{2}\right) , \quad \mathcal{M}_A^{(2)} = \frac{2\pi}{N_c q^2} N_c 4q^2 \beta^2 , \quad (4.4)$$

where ρ is defined in (3.3) and

$$\beta = \sqrt{1 - \rho} . \quad (4.5)$$

Multiplying eq. (4.4) by the 2-body phase space $\beta/(8\pi)$ we get the zeroth-order total cross section

$$T_V^{(2)} = \beta \left(1 + \frac{\rho}{2}\right) , \quad T_A^{(2)} = \beta^3 . \quad (4.6)$$

Thus, our choice for the normalization factor in eq. (4.2) is such that, in the massless limit, $T_V^{(2)} = T_A^{(2)} = 1$.

4.2 $Q\bar{Q}g$ cross section at order α_s

This is obtained starting from the amplitude

$$\mathcal{A}_{V/A}^{\mu\sigma} = \bar{u}(p) \left[\gamma^\sigma \frac{\not{p} + \not{k} + m}{(p+k)^2 - m^2} \Gamma_{V/A}^\mu + \Gamma_{V/A}^\mu \frac{\not{p} - \not{q} + m}{(p-q)^2 - m^2} \gamma^\sigma \right] v(p') . \quad (4.7)$$

We define

$$M_{V/A}^{\sigma\sigma'} = \left(-g_{\mu\nu} + \frac{q_\mu q_\nu}{q^2} \right) \sum \mathcal{A}_{V/A}^{\mu\sigma} \mathcal{A}_{V/A}^{*\nu\sigma'} \quad (4.8)$$

where the sum refers to the spin of the fermions in the final state.

The sum over the gluon polarization is

$$M_{V/A} = -g_{\sigma\sigma'} M_{V/A}^{\sigma\sigma'} . \quad (4.9)$$

We will need $M_{V/A}$ in $d = 4 - 2\epsilon$ dimensions. We have

$$\begin{aligned} M_V = & 8 \frac{x_1^2 + x_2^2}{(1-x_1)(1-x_2)} + \frac{16}{(1-x_1)^2(1-x_2)^2} \left(\frac{m^2}{q^2} \right) \left[2x_1x_2(x_1 + x_2) \right. \\ & \left. - 3(x_1^2 + x_2^2) - 8(1-x_1)(1-x_2) + 2 \right] - \frac{32}{(1-x_1)^2(1-x_2)^2} \left(\frac{m^2}{q^2} \right)^2 x_g^2 \\ & - \frac{16\epsilon}{(1-x_1)(1-x_2)} \left[x_1^2 + x_2^2 + (1-x_1)(1-x_2) + x_g - 1 \right. \\ & \left. - \left(\frac{m^2}{q^2} \right) \frac{x_g^2}{(1-x_1)(1-x_2)} \right] + \frac{8\epsilon^2}{(1-x_1)(1-x_2)} x_g^2 , \end{aligned} \quad (4.10)$$

and

$$\begin{aligned} M_A = & 8 \frac{x_1^2 + x_2^2}{(1-x_1)(1-x_2)} + \frac{16}{(1-x_1)^2(1-x_2)^2} \left(\frac{m^2}{q^2} \right) \left[-12(x_1 + x_2 - 2x_1x_2) \right. \\ & - 11x_1x_2(x_1 + x_2) + 8(x_1^2 + x_2^2) + x_1^3(x_2 - 1) + x_2^3(x_1 - 1) \\ & \left. + 2x_1^2x_2^2 + 4 \right] (1-\epsilon) + \frac{64}{(1-x_1)^2(1-x_2)^2} \left(\frac{m^2}{q^2} \right)^2 x_g^2 (1-\epsilon) \\ & + \frac{8\epsilon^2}{(1-x_1)(1-x_2)} x_g^2 , \end{aligned} \quad (4.11)$$

where x_1, x_2 and x_g are defined by (3.8) and (3.11). The three-body, order- α_s cross section is given by

$$\mathcal{M}_{V/A}^{(b)} = \frac{2\pi}{q^2} C_F g_s^2 \mu^{2\epsilon} M_{V/A} ,$$

where μ is the mass parameter of dimensional regularization and $C_F = \frac{N_c^2 - 1}{2N_c} = \frac{4}{3}$ for an SU(3) gauge theory.

We introduce a unit, purely space-like vector j lying in the event plane (i.e. the plane defined by \vec{p} , \vec{p}' and \vec{k}), and orthogonal to k

$$j \cdot q = 0, \quad j \cdot k = 0, \quad j^2 = -1. \quad (4.12)$$

$M_{V/A}^{\sigma\sigma'}$ has the general form

$$M_{V/A}^{\sigma\sigma'} = M_{V/A}^{\perp} g^{\sigma\sigma'} + M_{V/A}^j j^{\sigma} j^{\sigma'} + \text{terms involving } q \text{ or } k. \quad (4.13)$$

In the following, we will need $M_{V/A}^j$, but only in four dimensions

$$\begin{aligned} M_{V/A}^j = & \frac{2c_{V/A}}{(1-x_1)^2(1-x_2)^2} \left[4x_1x_2(x_1+x_2) - \rho(x_1+x_2)^2 - 4(x_1^2+x_2^2) \right. \\ & \left. - 12x_1x_2 + 4(\rho+2)(x_1+x_2) - 4(\rho+1) \right], \end{aligned} \quad (4.14)$$

where

$$c_V = \rho + 2 \quad c_A = -2(\rho - 1). \quad (4.15)$$

We also define, consistently with our previous notation

$$\mathcal{M}_{V/A}^{(b)\sigma\sigma'} = \frac{2\pi}{q^2} C_F g_s^2 \mu^{2\epsilon} M_{V/A}^{\sigma\sigma'}, \quad \mathcal{M}_{V/A}^{(b)\perp/j} = \frac{2\pi}{q^2} C_F g_s^2 \mu^{2\epsilon} M_{V/A}^{\perp/j}. \quad (4.16)$$

In the cases when the V/A suffix needs not be specified, we will simply write $\mathcal{M}_b^{\sigma\sigma'}$, \mathcal{M}_b^{\perp} and \mathcal{M}_b^j .

4.3 Virtual contributions

Corrections to the three-jet decay rate to order α_s^2 come from the interference of the one-loop graphs with the tree-level ones. These terms have been computed in $d = 4 - 2\epsilon$ dimensions. The algebra has been carried out in a straightforward way, using a MACSYMA program, which reduces the original Feynman graphs to a linear combination of scalar, one-loop integrals. The scalar integrals have been computed analytically. Their values are listed in Appendix E. Loop corrections to on-shell external lines require particular attention. First of all, gluon and light fermions self-energy corrections to external gluon lines vanish in dimensional regularization. Only the corrections coming from a heavy-flavour loop need be considered. We proceed

as follows. We compute the self-energy correction for a gluon propagator of small virtuality. We obtain, for the corrected propagator,

$$\frac{-ig_{\mu\nu}}{k^2} - N_\epsilon T_F g_s^2 \left(\frac{\mu^2}{m^2} \right)^\epsilon \frac{4}{3\epsilon} \frac{-i(g_{\mu\nu} - k_\mu k_\nu/k^2)}{k^2} + \frac{\mathcal{O}(k^2)}{k^2}, \quad (4.17)$$

where

$$N_\epsilon = \frac{(4\pi)^\epsilon}{(4\pi)^2} \Gamma(1 + \epsilon) \quad (4.18)$$

and the colour factor $T_F = 1/2$.

From this equation we immediately infer that the contribution to \mathcal{M}_v coming from the self-energy correction to the external gluon line amounts to

$$- N_\epsilon T_F g_s^2 \left(\frac{\mu^2}{m^2} \right)^\epsilon \frac{4}{3\epsilon} \times \mathcal{M}_b. \quad (4.19)$$

A similar consideration applies to the self-energy corrections to heavy-flavour external lines. In this case one finds

$$\frac{i}{\not{p} - m} - N_\epsilon C_F g_s^2 \left(\frac{\mu^2}{m^2} \right)^\epsilon \left(\frac{3}{\epsilon} + 4 \right) \frac{i}{\not{p} - m} - \frac{i}{\not{p} - m} i\delta m \frac{i}{\not{p} - m} + \frac{\mathcal{O}(p^2 - m^2)}{\not{p} - m}, \quad (4.20)$$

where

$$\delta m = N_\epsilon C_F g_s^2 \left(\frac{\mu^2}{m^2} \right)^\epsilon m \left(\frac{3}{\epsilon} + 4 \right). \quad (4.21)$$

The infinite mass correction should be removed by the mass counterterm. We define the Feynman rule for the mass counterterm to be given by an insertion of $-im_c$ in the fermion propagator, where

$$m_c = -\delta m = -N_\epsilon C_F g_s^2 \left(\frac{\mu^2}{m^2} \right)^\epsilon m \left(\frac{3}{\epsilon} + 4 \right). \quad (4.22)$$

This precisely cancels the δm term in eq. (4.20), so that the pole of the propagator is not displaced by radiative corrections, and m corresponds to the pole mass definition. Thus, the effect of the fermion self-energy correction to an external line, including the effect of the mass counterterm, is given by

$$- N_\epsilon C_F g_s^2 \left(\frac{\mu^2}{m^2} \right)^\epsilon \left(\frac{3}{\epsilon} + 4 \right) \times \mathcal{M}_b. \quad (4.23)$$

To complete the computation of virtual corrections, the diagrams with a mass counterterm insertion in internal fermion lines should also be included. After that, charge

renormalization is all that is needed, since we are computing a physical cross section. We carry out the charge renormalization in the mixed scheme of ref. [14], in which the light flavours n_{lf} are subtracted in the $\overline{\text{MS}}$ scheme, while the heavy-flavour loops are subtracted at zero momentum. In this scheme the heavy flavour decouples at low energy. The prescription for charge renormalization in this scheme is

$$\alpha_s \rightarrow \alpha_s \left\{ 1 + g_s^2 N_\epsilon \left[\left(\frac{4}{3\epsilon} T_F n_{\text{lf}} - \frac{11}{3\epsilon} C_A \right) + \left(\frac{\mu^2}{m^2} \right)^\epsilon \frac{4}{3\epsilon} T_F \right] \right\}, \quad (4.24)$$

where $C_A = N_c = 3$ for an SU(3) gauge theory. It amounts to adding the following correction to our virtual term

$$g_s^2 N_\epsilon \left[\left(\frac{4}{3\epsilon} T_F n_{\text{lf}} - \frac{11}{3\epsilon} C_A \right) + \left(\frac{\mu^2}{m^2} \right)^\epsilon \frac{4}{3\epsilon} T_F \right] \times \mathcal{M}_b. \quad (4.25)$$

Observe that in this scheme the term corresponding to the heavy-flavour loop compensates exactly the self-energy correction to the external gluon line, coming from the heavy-flavour loop. This is easily understood: the final-state gluon is on the mass shell, so it is effectively renormalized at zero momentum by the heavy quark loop, and thus decoupling applies. We can now resume the combined effect of external line corrections and renormalization to be included with \mathcal{M}_v

$$N_\epsilon g_s^2 \left(\frac{\mu^2}{m^2} \right)^\epsilon \left\{ -2C_F \left(\frac{3}{\epsilon} + 4 \right) + \left(\frac{4}{3\epsilon} T_F n_{\text{lf}} - \frac{11}{3\epsilon} C_A \right) \left(\frac{\mu^2}{m^2} \right)^{-\epsilon} \right\} \times \mathcal{M}_b. \quad (4.26)$$

The factor of 2 in front of the fermion external line corrections is to account for the two fermion lines.

4.4 Soft and collinear limit of the $Q\overline{Q}gg$ and $Q\overline{Q}q\bar{q}$ cross sections

Here we derive an expression for the singular part of the four-body cross section, valid in both the collinear and the soft limit. These limits are both characterized by $y \rightarrow 0$, except that in the soft limit, at the same time $v \rightarrow 0$ ($l \rightarrow 0$) or $v \rightarrow 1$ ($k \rightarrow 0$). We will focus our discussion on the $Q\overline{Q}gg$ final state. The other process $Q\overline{Q}q\bar{q}$ is much simpler, since only collinear singularities are present there. Since the same formulae apply irrespective of the vector or axial case, we will always drop the V/A suffix.

We begin with the soft singularities of \mathcal{M}_{gg} . They are given by eq. (D.5), which we now rewrite

$$\mathcal{M}_{gg}^{\text{soft}} \sim g_s^2 \mu^{2\epsilon} \left\{ C_A \left[\frac{p \cdot k}{(p \cdot l)(k \cdot l)} + \frac{p' \cdot k}{(p' \cdot l)(k \cdot l)} \right] + 2 \left(C_F - \frac{C_A}{2} \right) \frac{p \cdot p'}{(p \cdot l)(p' \cdot l)} \right\}$$

$$- C_F \left[\frac{m^2}{(p \cdot l)^2} + \frac{m^2}{(p' \cdot l)^2} \right] + (k \leftrightarrow l) \} \times \mathcal{M}_b . \quad (4.27)$$

From Section 3, we can derive an approximation of the scalar products in the limit of l soft

$$\frac{p \cdot k}{(p \cdot l)(k \cdot l)} \sim \frac{2h}{q^2} \frac{1}{y[y + h v]} \equiv E_{p,k;l}(x_1, x_2, y, v)$$

$$\frac{p \cdot p'}{(p \cdot l)(p' \cdot l)} \sim \frac{K}{m^2} \frac{1}{y + h v} \frac{1}{y - c \cos \phi \sqrt{y} \sqrt{v} + g v} \equiv E_{p,p';l}(x_1, x_2, y, v, \phi)$$

$$\frac{m^2}{(p \cdot l)^2} \sim \frac{4h}{q^2} \frac{1}{[y + h v]^2} \equiv E_{p,p;l}(x_1, x_2, y, v) ,$$

where

$$h = \frac{q^2}{m^2} (1 - x_2)^2$$

$$a = \frac{2}{(1 - x_1)(1 - x_2)} \left\{ x_1 + x_2 - 1 - \frac{m^2}{q^2} \left[2 + \frac{1 - x_2}{1 - x_1} + \frac{1 - x_1}{1 - x_2} \right] \right\}$$

$$b = \frac{2}{(1 - x_1)(1 - x_2)} \left\{ x_1 + x_2 - 1 - \frac{m^2}{q^2} \left[2 + \frac{1 - x_1}{1 - x_2} \right] \right\}$$

$$K = \frac{1 - x_2}{1 - x_1} \frac{4}{b} \left[x_1 + x_2 - 1 - \frac{2m^2}{q^2} \right]$$

$$c = \frac{2\sqrt{2a}}{b}$$

$$g = \frac{2}{b} .$$

We will also need analogous formulae in the variables in which the roles of p and p' are interchanged. We have

$$\frac{p' \cdot k}{(p' \cdot l)(k \cdot l)} \sim E'_{p',k;l}(x_1, x_2, y, v') \equiv E_{p,k;l}(x_2, x_1, y, v')$$

$$\frac{p \cdot p'}{(p \cdot l)(p' \cdot l)} \sim E'_{p,p';l}(x_1, x_2, y, v', \phi') \equiv E_{p,p';l}(x_2, x_1, y, v', \phi')$$

$$\frac{m^2}{(p' \cdot l)^2} \sim E'_{p',p';l}(x_1, x_2, y, v') \equiv E_{p',p';l}(x_2, x_1, y, v') .$$

Soft factors for the case when k is soft are instead obtained from the above using eqs. (3.16). For example

$$\begin{aligned} E_{p,l;k}(x_1, x_2, y, v) &= E_{p,k;l}(x_1, x_2, y, 1-v) , \\ E_{p,p';k}(x_1, x_2, y, v) &= E_{p,p';l}(x_1, x_2, y, 1-v, \phi + \pi) . \end{aligned} \quad (4.28)$$

We can now write down our approximate soft cross section. We have

$$\begin{aligned} \mathcal{M}_{gg}^{\text{soft}} &= g_s^2 \mu^{2\epsilon} \left\{ C_A \left[E_{p,k;l} + E'_{p',k;l} + E_{p,l;k} + E'_{p',l;k} \right] \right. \\ &\quad + (C_F - C_A/2) \left[E_{p,p';l} + E'_{p,p';l} + E_{p,p';k} + E'_{p,p';k} \right] \\ &\quad \left. - C_F \left[E_{p,p;l} + E'_{p',p';l} + E_{p,p;k} + E'_{p',p';k} \right] \right\} \times \mathcal{M}_b . \end{aligned} \quad (4.29)$$

The soft cross section written in this way is symmetric under the interchange of k and l , and of p and p' .

The collinear part of the cross section receives contributions from both the gg and the $q\bar{q}$ final state. For the gg contribution, according to eq. (B.10), we can write the collinear part

$$\begin{aligned} g_s^2 \mu^{2\epsilon} \frac{4C_A}{q^2 y} &\left\{ - \left[-2 + \frac{1}{z} + \frac{1}{1-z} + z(1-z) \right] g_{\sigma\sigma'} \right. \\ &\quad \left. - 2z(1-z)(1-\epsilon) \left[\frac{k_{\perp\sigma} k_{\perp\sigma'}}{k_{\perp}^2} - \frac{g_{\perp\sigma\sigma'}}{2-2\epsilon} \right] \right\} \times \mathcal{M}_b^{\sigma\sigma'} , \end{aligned} \quad (4.30)$$

where z is the momentum fraction of l versus $l+k$ in the collinear limit. It can be chosen to be equal to v or to v' .

The perpendicular direction refers instead to a direction orthogonal to $l+k$ in the centre-of-mass system and in the collinear limit. Using eq. (4.13), the azimuth-dependent term of (4.30) becomes

$$\begin{aligned} g_s^2 \mu^{2\epsilon} \frac{4C_A}{q^2 y} &\left\{ - 2z(1-z)(1-\epsilon) \left[\mathcal{M}_b^{\perp} + \mathcal{M}_b^j \frac{(k_{\perp} \cdot j)^2}{k_{\perp}^2} - \frac{\mathcal{M}_b^{\perp}(2-2\epsilon) - \mathcal{M}_b^j}{2-2\epsilon} \right] \right\} \\ &= g_s^2 \mu^{2\epsilon} \frac{4C_A}{q^2 y} \left\{ - z(1-z) \mathcal{M}_b^j \left[\frac{(k_{\perp} \cdot j)^2}{k_{\perp}^2} 2(1-\epsilon) + 1 \right] \right\} . \end{aligned} \quad (4.31)$$

It is now easy to show that, in the collinear limit, $(k_{\perp} \cdot j)^2/k_{\perp}^2 \rightarrow -\cos^2 \phi$.

Part of the collinear singularities are already contained in the soft-limit expression. In fact, for $y \rightarrow 0$ at v fixed, we have

$$E_{p,k;l} \approx E'_{p',k;l} \approx \frac{2}{q^2 y v}, \quad E_{p,l;k} \approx E'_{p',l;k} \approx \frac{2}{q^2 y (1-v)}. \quad (4.32)$$

Thus, the $1/z$ and $1/(1-z)$ terms in the collinear limit formula (4.30) should not be included, since they are already present in the soft term. We thus arrive at the following expression for the collinear term to be added to the soft term

$$\begin{aligned} \mathcal{M}_{gg}^{\text{coll}} = g_s^2 \mu^{2\epsilon} \frac{4C_A}{q^2 y} & \left\{ \mathcal{M}_b \left[\frac{v(1-v) + v'(1-v')}{2} - 2 \right] \right. \\ & \left. + \frac{\mathcal{M}_b^j}{2} \left[v(1-v) \left(2(1-\epsilon) \cos^2 \phi - 1 \right) + v'(1-v') \left(2(1-\epsilon) \cos^2 \phi' - 1 \right) \right] \right\} \end{aligned} \quad (4.33)$$

An analogous procedure yields an expression for the collinear part of $\mathcal{M}_{q\bar{q}}$ (see eq. (C.2))

$$\begin{aligned} \mathcal{M}_{q\bar{q}}^{\text{coll}} = g_s^2 \mu^{2\epsilon} \frac{4n_{\text{lf}} T_F}{q^2 y} & \left\{ \mathcal{M}_b \frac{1}{4(1-\epsilon)} \left[v'^2 + (1-v')^2 + v^2 + (1-v)^2 - 2\epsilon \right] \right. \\ & \left. - \frac{\mathcal{M}_b^j}{2} \left[v(1-v) \left(2 \cos^2 \phi - \frac{1}{1-\epsilon} \right) + v'(1-v') \left(2 \cos^2 \phi' - \frac{1}{1-\epsilon} \right) \right] \right\}. \end{aligned} \quad (4.34)$$

The expressions $\mathcal{M}_{gg}^{\text{coll}}$, $\mathcal{M}_{q\bar{q}}^{\text{coll}}$ and $\mathcal{M}_{gg}^{\text{soft}}$ depend upon x_1 and x_2 via \mathcal{M}_b and \mathcal{M}_b^j . These expressions are meaningful only if x_1 and x_2 belong to the domain of the three-body phase space. We thus define

$$\begin{aligned} \widetilde{\mathcal{M}}_{gg} &= (\mathcal{M}_{gg}^{\text{soft}} + \mathcal{M}_{gg}^{\text{coll}}) \theta_3(x_1, x_2), \\ \widetilde{\mathcal{M}}_{q\bar{q}} &= \mathcal{M}_{q\bar{q}}^{\text{coll}} \theta_3(x_1, x_2), \end{aligned} \quad (4.35)$$

where the θ_3 function is precisely defined to be zero when x_1 and x_2 are outside the three-body phase-space region. More specifically, using the definitions of eqs. (3.12)

$$\theta_3(x_1, x_2) = \theta(1-x_1) \theta(x_1 - \sqrt{\rho}) \theta(x_{2+} - x_2) \theta(x_2 - x_{2-}). \quad (4.36)$$

We are now in a position to specify the subtraction procedure outlined in Section 2. Our expression for the second-order contribution to an infrared- and collinear-safe quantity G is given by

$$\begin{aligned} \frac{1}{2} \int \mathcal{M}_{gg}(x_1, x_2, y, v, \phi) G(x_1, x_2, y, v, \phi) d\phi_4 \\ + \int \mathcal{M}_{q\bar{q}}(x_1, x_2, y, v, \phi) G(x_1, x_2, y, v, \phi) d\phi_4 + \int \mathcal{M}_v(x_1, x_2) G(x_1, x_2) d\phi_3, \end{aligned}$$

where all quantities are computed in $d = 4 - 2\epsilon$ dimensions. The factor $1/2$ in front of the gg contribution accounts for the two identical gluons in the final state. We rewrite the above expression as

$$\begin{aligned} & \frac{1}{2} \int \left(\mathcal{M}_{gg}(x_1, x_2, y, v, \phi) G(x_1, x_2, y, v, \phi) - \widetilde{\mathcal{M}}_{gg}(x_1, x_2, y, v, \phi) G(x_1, x_2) \right) d\Phi_4 \\ & + \int \left(\mathcal{M}_{q\bar{q}}(x_1, x_2, y, v, \phi) G(x_1, x_2, y, v, \phi) - \widetilde{\mathcal{M}}_{q\bar{q}}(x_1, x_2, y, v, \phi) G(x_1, x_2) \right) d\Phi_4 \\ & + \int \left(\mathcal{M}_v(x_1, x_2) + \widetilde{\mathcal{M}}_i(x_1, x_2) \right) G(x_1, x_2) d\Phi_3 \end{aligned} \quad (4.37)$$

where we have defined

$$\widetilde{\mathcal{M}}_i(x_1, x_2) = \frac{1}{2} \int \widetilde{\mathcal{M}}_{gg}(x_1, x_2, y, v, \phi) d\Phi_{4/3} + \int \widetilde{\mathcal{M}}_{q\bar{q}}(x_1, x_2, y, v, \phi) d\Phi_{4/3} \quad (4.38)$$

and $d\Phi_{4/3}$ is defined by

$$d\Phi_4 \theta_3(x_1, x_2) = d\Phi_{4/3} d\Phi_3. \quad (4.39)$$

An explicit expression for $d\Phi_{4/3}$ can be obtained from eqs. (3.13) and (3.4). We first notice that the four-body phase space is almost proportional to the three-body phase space, except for the ratio

$$\left(\frac{4(x_1^2 - \rho)(x_2^2 - \rho) - [(x_g^2 - 4y) - (x_1^2 - \rho) - (x_2^2 - \rho)]^2}{4(x_1^2 - \rho)(x_2^2 - \rho) - [x_g^2 - (x_1^2 - \rho) - (x_2^2 - \rho)]^2} \right)^{-\epsilon} = 1 + \mathcal{O}(y\epsilon). \quad (4.40)$$

On the other hand, terms of order $y\epsilon$ can be neglected, since they cannot generate infrared singularities, because of the y factor, and therefore they can only produce terms of order ϵ . Thus we can write

$$d\Phi_{4/3} = N_\epsilon R_\epsilon q^2 q^{-2\epsilon} \int_0^{y+} dy y^{-\epsilon} \int_0^1 dv [v(1-v)]^{-\epsilon} \frac{1}{N_\phi} \int_0^\pi d\phi (\sin \phi)^{-2\epsilon} \quad (4.41)$$

or the analogous one in the v', ϕ' variables. The normalization factor N_ϵ is defined in (4.18), while

$$R_\epsilon = \frac{1}{\Gamma(1+\epsilon)\Gamma(1-\epsilon)} = 1 - \frac{\pi^2 \epsilon^2}{6} + \mathcal{O}(\epsilon^3).$$

Since we are free to choose the set of variables we prefer in the $d\Phi_{4/3}$ integration, it is easy to see that the $\widetilde{\mathcal{M}}_i(x_1, x_2)$ term reduces to

$$\begin{aligned} \widetilde{\mathcal{M}}_i(x_1, x_2) &= g_s^2 \mu^{2\epsilon} \int \left\{ \frac{1}{2} \frac{4C_A}{q^2 y} (v(1-v) - 2) \right. \\ &+ \frac{2n_{\text{lf}} T_F}{q^2 y} \frac{1}{1-\epsilon} [v^2 + (1-v)^2 - \epsilon] \\ &+ \left. \frac{1}{2} [4C_A E_{p,k;l} + 4(C_F - C_A/2) E_{p,p';l} - 4C_F E_{p,p;l}] \right\} \times \mathcal{M}_b d\Phi_{4/3} \end{aligned}$$

where the term proportional to \mathcal{M}^j has been dropped, since it vanishes in $d = 4 - 2\epsilon$ dimensions, after the azimuthal integration.

Furthermore, the remaining collinear term is easily integrated. We define

$$\begin{aligned} I_{gg}^{\text{coll}} &= \int_0^{y_+} dy y^{-\epsilon} \int_0^1 dv [v(1-v)]^{-\epsilon} \frac{1}{N_\phi} \int_0^\pi d\phi (\sin \phi)^{-2\epsilon} \frac{1}{y} [v(1-v) - 2] = \\ &= -\frac{1}{\epsilon} [1 - \epsilon \log(y_+)] \left(-\frac{11}{6} - \frac{67}{18}\epsilon \right) + \mathcal{O}(\epsilon) \end{aligned} \quad (4.42)$$

and

$$\begin{aligned} I_{q\bar{q}}^{\text{coll}} &= \int_0^{y_+} dy y^{-\epsilon} \int_0^1 dv [v(1-v)]^{-\epsilon} \frac{1}{N_\phi} \int_0^\pi d\phi (\sin \phi)^{-2\epsilon} \frac{1}{y} \frac{v^2 + (1-v)^2 - \epsilon}{1 - \epsilon} = \\ &= -\frac{1}{\epsilon} [1 - \epsilon \log(y_+)] \left(\frac{2}{3} + \frac{10}{9}\epsilon \right) + \mathcal{O}(\epsilon) . \end{aligned} \quad (4.43)$$

For the integrals of the soft term we define

$$I_{p,k;l} = q^2 \int_0^{y_+} dy y^{-\epsilon} \int_0^1 dv [v(1-v)]^{-\epsilon} \frac{1}{N_\phi} \int_0^\pi d\phi (\sin \phi)^{-2\epsilon} E_{p,k;l}$$

and the analogous ones for $I_{p,p;l}$ and $I_{p,p';l}$. In this way

$$I_{p,k;l} = 2h I_1 \quad I_{p,p;l} = 4h I_2 \quad I_{p,p';l} = K \frac{q^2}{m^2} I_3 ,$$

where the values of I_1 , I_2 and I_3 are collected in Appendix F.

Our final expression for $\widetilde{\mathcal{M}}_i(x_1, x_2)$ is therefore

$$\begin{aligned} \widetilde{\mathcal{M}}_i(x_1, x_2) &= N_\epsilon R_\epsilon g_s^2 \left(\frac{\mu^2}{q^2} \right)^\epsilon \left\{ 2C_A I_{gg}^{\text{coll}} + 2n_{\text{lf}} T_F I_{q\bar{q}}^{\text{coll}} \right. \\ &\quad \left. + \left[2C_A I_{p,k;l} + 2(C_F - C_A/2) I_{p,p';l} - 2C_F I_{p,p;l} \right] \right\} \times \mathcal{M}_b . \end{aligned}$$

5 Checks of the calculation

Several checks have been performed to control the correctness of our results.

1. The divergences coming from UV and IR poles all cancel.
2. The full calculation, as $m \rightarrow 0$, agrees with the massless result of ref. [1].

3. Our four-dimensional matrix elements for the processes $e^+e^- \rightarrow Z/\gamma \rightarrow Q\bar{Q}gg$ and $e^+e^- \rightarrow Z/\gamma \rightarrow Q\bar{Q}Q\bar{Q}$ agree with ref. [10]. Furthermore, the soft and collinear limits of the four-body matrix elements for the process $Z/\gamma \rightarrow Q\bar{Q}$ plus two light partons are correctly given by formulae (4.35).
4. Near the production threshold, we should recover the Coulomb singularity. If β is the velocity of the two massive quarks in the fermion centre-of-mass system, then (see ref. [15])

$$d\sigma_{V/A}^{(v)}(x_1, x_2) \xrightarrow{\beta \rightarrow 0} \frac{\pi^2}{\beta} \left(C_F - \frac{C_A}{2} \right) d\sigma_{V/A}^{(b)}(x_1, x_2). \quad (5.1)$$

By evaluating $(p+p')^2$ in the centre of mass of the two massive quarks, for small β , we get

$$(p+p')^2 = \left[2 \left(m + \frac{m}{2} \beta^2 + \mathcal{O}(\beta^4) \right) \right]^2 = (q-k)^2 = q^2 (x_1 + x_2 - 1). \quad (5.2)$$

Choosing for example $x_1 = x_2$ we have

$$x_1 = x_2 = \frac{1}{2} (1 + \rho + \rho \beta^2).$$

By letting β get smaller and smaller we have checked that the behaviour of the virtual differential cross section is in agreement with eq. (5.1).

A further check is described in detail in ref. [16].

6 Conclusion

In this paper we have described a next-to-leading-order calculation of the heavy-flavour production cross section in e^+e^- collisions, including quark mass effects. Some applications of our calculation have appeared in the literature [5], [16].

We have used a subtraction method instead of a slicing method, in order to avoid having to worry about taking the limit of some small parameters. We have performed several checks on the correctness of our results. Among them, the small mass limit of the energy-energy correlation is of particular significance, since, for this quantity, some discrepancies among different approaches are still present (see ref. [17]).

Appendix A: Phase space for four massive quarks

For completeness, we describe in this appendix the phase space for four massive quarks in the final state. The process is

$$e^+(p'_e) + e^-(p_e) \rightarrow Z/\gamma(q) \rightarrow Q(p) + \bar{Q}(p') + Q(r) + \bar{Q}(r') , \quad (\text{A.1})$$

where

$$r^2 = r'^2 = p^2 = p'^2 = m^2 .$$

The four-body phase space is obtained with a procedure similar to the one given in Section 3, with the simplification that now the entire cross section has no infrared or collinear divergences, so that we can put ourselves directly in $d = 4$ dimensions and we do not need to divide the phase-space region into two different pieces. In the centre-of-mass frame of one heavy quark-antiquark pair we have

$$r = (r_0, |\mathbf{r}| \sin \theta \sin \phi, |\mathbf{r}| \sin \theta \cos \phi, |\mathbf{r}| \cos \theta)$$

$$r' = (r_0, -|\mathbf{r}| \sin \theta \sin \phi, -|\mathbf{r}| \sin \theta \cos \phi, -|\mathbf{r}| \cos \theta)$$

$$p = p_0 \left(1, 0, 0, \sqrt{1 - \frac{m^2}{p_0^2}} \right)$$

$$p' = p'_0 \left(1, 0, \sqrt{1 - \frac{m^2}{p_0'^2}} \sin \alpha, \sqrt{1 - \frac{m^2}{p_0'^2}} \cos \alpha \right) ,$$

where

$$y = \frac{(r + r')^2}{q^2} \implies r_0 = \sqrt{q^2} \frac{\sqrt{y}}{2}$$

and p_0 , p'_0 and $\cos \alpha$ are given by (3.9) and (3.10), while $|\mathbf{r}| = \sqrt{r_0^2 - m^2}$.

The four-body phase space is given by

$$(\text{PS})^{(4)} = \frac{q^4}{(4\pi)^6} \int_{\rho}^{\bar{y}_+} dy \sqrt{1 - \frac{\rho}{y}} \int_{\sqrt{\rho}}^{\bar{x}_{1+}} dx_1 \int_{\bar{x}_{2-}}^{\bar{x}_{2+}} dx_2 \int_0^1 dv \int_0^{2\pi} d\phi , \quad (\text{A.2})$$

where

$$\begin{aligned} \bar{y}_+ &= (1 - \sqrt{\rho})^2 \\ \bar{x}_{1+} &= 1 - y - \sqrt{\rho y} \\ \bar{x}_{2\pm} &= \frac{1}{4(1 - x_1) + \rho} \left[(2 - x_1)(2 + \rho - 2y - 2x_1) \right. \\ &\quad \left. \pm 2 \sqrt{(x_1^2 - \rho) [(x_1 - 1 + y)^2 - \rho y]} \right] . \end{aligned} \quad (\text{A.3})$$

A statistical factor $1/(2!2!) = 1/4$ must be supplied to (A.2), because of the presence of two pairs of identical particles in the final state.

Appendix B: Collinear limit for $g \rightarrow gg$ splitting

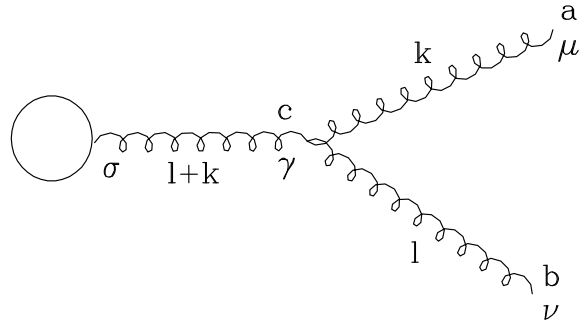


Figure 6: *Gluon splitting*

In this appendix we will derive the singular part of the square of the invariant amplitude when two collinear gluons are produced. In the collinear limit, the amplitude for the emission of two gluons in the final state can be decomposed into two parts: the first one contains the graphs where the two gluons are emitted by a single virtual one (see Fig. 6), and the other one contains all the other graphs

$$\mathcal{A}^{ab} = \left\{ \mathcal{A}_c^\sigma(l+k) \frac{iP_{\sigma\gamma}(k+l)}{(k+l)^2} (-g_s) f^{abc} \Gamma^{\mu\nu\gamma}(-k, -l, k+l) + \mathcal{R}_{ab}^{\mu\nu} \right\} \epsilon_\mu(k) \bar{\epsilon}_\nu(l) , \quad (B.1)$$

where a and b are the colour indices of the final gluons, P is the spin projector of the gluon propagator, g_s is the strong coupling constant, f^{abc} are the structure constants of the SU(3) gauge group, ϵ and $\bar{\epsilon}$ are the polarization vectors of the final gluons, and $\Gamma^{\mu\nu\gamma}$ is the Lorentz part of the three-gluon vertex

$$\Gamma^{\mu\nu\gamma}(-k, -l, k+l) = (-k+l)^\gamma g^{\mu\nu} + (-2l-k)^\mu g^{\nu\gamma} + (2k+l)^\nu g^{\mu\gamma} . \quad (B.2)$$

Only the first term of (B.1) is singular in the collinear limit. We want to stress the fact that this term is singular in the soft limit too. Therefore one has to be careful, when considering the soft and collinear limit of the square amplitude, not to include this contribution twice.

We introduce two light-like vectors

$$\begin{aligned} t &= \left(|\vec{k} + \vec{l}|, \vec{k} + \vec{l} \right) \\ \eta &= c \times \left(\frac{1}{|\vec{k} + \vec{l}|}, -\frac{\vec{k} + \vec{l}}{|\vec{k} + \vec{l}|^2} \right) \end{aligned} \quad (\text{B.3})$$

and choose $c = 1/4$, so that $2t \cdot \eta = 1$. We then decompose

$$l^\mu + k^\mu = t^\mu + \xi \eta^\mu, \quad (\text{B.4})$$

where

$$\xi = (l + k)^2 = q^2 y.$$

We will work in the light-cone gauge, characterized by the light-like vector η , because, in this gauge (as we will see), the interference of the divergent term of (B.1) and of the finite term \mathcal{R} does not contribute to the singular part.

The gluon spin projector is then written

$$P^{\sigma\gamma}(p) = -g^{\sigma\gamma} + \frac{\eta^\sigma p^\gamma + \eta^\gamma p^\sigma}{\eta \cdot p}. \quad (\text{B.5})$$

We write l and k as

$$\begin{aligned} k^\mu &= v t^\mu + \xi' \eta^\mu + k_\perp^\mu \\ l^\mu &= (1 - v) t^\mu + \xi'' \eta^\mu - k_\perp^\mu, \end{aligned} \quad (\text{B.6})$$

with k_\perp such that $t \cdot k_\perp = \eta \cdot k_\perp = 0$. By imposing that $k^2 = l^2 = 0$ and that $(l + k)^2 = q^2 y$ we have

$$k_\perp^2 = -v(1 - v) q^2 y \quad \xi' = (1 - v) q^2 y \quad \xi'' = v q^2 y.$$

From (B.4) and (B.6) we finally obtain

$$\begin{aligned} k^\mu &= \frac{1}{1 - v} \left[v l^\mu + (1 - 2v) q^2 y \eta^\mu + k_\perp^\mu \right] \\ l^\mu &= \frac{1}{v} \left[(1 - v) k^\mu - (1 - 2v) q^2 y \eta^\mu - k_\perp^\mu \right]. \end{aligned} \quad (\text{B.7})$$

Considering that

$$(k + l)^\gamma P_{\sigma\gamma} = 2 q^2 y \eta_\sigma \quad k_\mu \epsilon^\mu(k) = 0 \quad l_\nu \bar{\epsilon}^\nu(l) = 0,$$

with the help of eq. (B.7) we can rewrite the amplitude (B.1)

$$\begin{aligned} \mathcal{A}^{ab} = & \left\{ \mathcal{A}_c^\sigma(l+k) \frac{iP_{\sigma\gamma}(k+l)}{q^2 y} (-g_s) f^{abc} \right. \\ & \left. \times \left[-2 k_\perp^\gamma g^{\mu\nu} + \frac{2}{v} k_\perp^\mu g^{\nu\gamma} + \frac{2}{1-v} k_\perp^\nu g^{\mu\gamma} + \mathcal{O}(y) \right] + \mathcal{R}_{ab}^{\mu\nu} \right\} \epsilon_\mu(k) \bar{\epsilon}_\nu(l) . \end{aligned}$$

Observe that the first term is of order $1/\sqrt{y}$, so that a singularity with strength $1/y$ can arise only from the square of the first term, and the interference term does not contribute. Furthermore, we can now substitute

$$\begin{aligned} \mathcal{A}_c^\sigma(l+k) \rightarrow & \mathcal{A}_c^\sigma(t) \equiv \text{tree-level amplitude} \\ P^{\sigma\gamma}(k+l) \rightarrow & P^{\sigma\gamma}(t) = -g^{\sigma\gamma} + \frac{\eta^\sigma t^\gamma + \eta^\gamma t^\sigma}{\eta \cdot t} \equiv -g_\perp^{\sigma\gamma} . \end{aligned}$$

Remembering that $\eta \cdot \epsilon = \eta \cdot \bar{\epsilon} = 0$, we can write \mathcal{A}^{ab} in the form

$$\mathcal{A}^{ab} = \mathcal{A}_{c\sigma}(t) \frac{g_2}{q^2 y} i f^{abc} \left[-2 k_\perp^\sigma g_\perp^{\mu\nu} + \frac{2}{v} k_\perp^\mu g_\perp^{\nu\sigma} + \frac{2}{1-v} k_\perp^\nu g_\perp^{\mu\sigma} \right] \epsilon_\mu(k) \bar{\epsilon}_\nu(l) , \quad (\text{B.8})$$

where only the term contributing to the singularity has been kept.

By squaring the amplitude and summing over the colours and spins of the final gluons, we obtain, for the collinear singular part

$$\begin{aligned} \mathcal{M}_{\text{gg}}^{\text{col}} = & \frac{g_s^2}{q^2} \frac{4C_A}{y} \left\{ - \left[-2 + \frac{1}{v} + \frac{1}{1-v} + v(1-v) \right] g_{\sigma\sigma'} \right. \\ & \left. - 2v(1-v)(1-\epsilon) \left[\frac{k_{\perp\sigma} k_{\perp\sigma'}}{k_\perp^2} - \frac{g_{\perp\sigma\sigma'}}{2-2\epsilon} \right] \right\} \mathcal{A}_c^\sigma(t) \mathcal{A}_c^{*\sigma'}(t) , \end{aligned} \quad (\text{B.9})$$

where we have used the gauge invariance $t_\sigma \mathcal{A}_c^\sigma(t) = 0$ to write the following identity

$$\mathcal{A}_c^\sigma(t) \mathcal{A}_c^{*\sigma'}(t) g_{\perp\sigma\sigma'} = \mathcal{A}_c^\sigma(t) \mathcal{A}_c^{*\sigma'}(t) g_{\sigma\sigma'} .$$

The first term of (B.9) is recognized to be the Altarelli-Parisi splitting function for the gluon-gluon process, in $d = 4 - 2\epsilon$ dimensions. The second term vanishes after azimuthal average in $4 - 2\epsilon$ dimensions.

Coming now to our problem, we can further specify the structure of $\mathcal{A}_c^\sigma(t) \mathcal{A}_c^{*\sigma'}(t)$. In fact, by using eq. (4.16), we can write (B.9) in the following form

$$\begin{aligned} \mathcal{M}_{\text{gg}}^{\text{col}} = & g_s^2 \mu^{2\epsilon} \frac{4C_A}{q^2 y} \left\{ - \left[-2 + \frac{1}{v} + \frac{1}{1-v} + v(1-v) \right] g_{\sigma\sigma'} \right. \\ & \left. - 2v(1-v)(1-\epsilon) \left[\frac{k_{\perp\sigma} k_{\perp\sigma'}}{k_\perp^2} - \frac{g_{\perp\sigma\sigma'}}{2-2\epsilon} \right] \right\} \times \mathcal{M}_b^{\sigma\sigma'} . \end{aligned} \quad (\text{B.10})$$

Appendix C: Collinear limit for $g \rightarrow q\bar{q}$ splitting

Following the same steps as in the previous appendix, we can give the approximation of the square of the amplitude in the limit of a collinear couple of massless quark-antiquark. The invariant amplitude is

$$\mathcal{A} = \mathcal{A}_c^\sigma(k+l) \frac{iP_{\rho\sigma}(k+l)\delta^{cc'}}{(k+l)^2} \bar{u}(k) \left(-ig_s \gamma^\rho t^{c'} \right) v(l) ,$$

where P is given by (B.5) and t^c are the generators of SU(3) gauge symmetry. By squaring this amplitude and summing over the spins and colours of the final quarks, we obtain

$$\mathcal{M}_{q\bar{q}}^{\text{col}} = \frac{T_F g_s^2}{q^4 y^2} \mathcal{A}_c^\sigma(k+l) \mathcal{A}_c^{*\sigma'}(k+l) P_{\rho\sigma}(k+l) P_{\rho'\sigma'}(k+l) \text{Tr} \left(\not{k} \gamma^\rho \not{l} \gamma^{\rho'} \right) ,$$

where t^c are normalized such that $\text{Tr} \left(t^a t^b \right) = T_F \delta^{ab}$.

Considering now eqs. (B.6), we see that, in the collinear limit, the trace is of the order of y , so that the singular part can be obtained by putting $y = 0$ in the rest of the numerator

$$\mathcal{M}_{q\bar{q}}^{\text{col}} = \frac{T_F g_s^2}{q^4 y^2} \mathcal{A}_c^\sigma(t) \mathcal{A}_c^{*\sigma'}(t) g_{\perp\rho\sigma} g_{\perp\rho'\sigma'} \text{Tr} \left(\not{k} \gamma^\rho \not{l} \gamma^{\rho'} \right) ,$$

where we have used the definition of t given in eq. (B.4). Evaluating the trace and keeping in the numerator only the terms proportional to y , we obtain

$$\mathcal{M}_{q\bar{q}}^{\text{col}} = \frac{T_F g_s^2}{q^4 y^2} 4 \left[-2k_{\perp\sigma} k_{\perp\sigma'} - \frac{q^2 y}{2} g_{\sigma\sigma'} \right] \mathcal{A}_c^\sigma(t) \mathcal{A}_c^{*\sigma'}(t) ,$$

that is

$$\begin{aligned} \mathcal{M}_{q\bar{q}}^{\text{col}} = & \frac{g_s^2}{q^2} \frac{4 T_F}{y} \left\{ -\frac{1}{2-2\epsilon} \left[v^2 + (1-v)^2 - \epsilon \right] g_{\sigma\sigma'} \right. \\ & \left. + 2v(1-v) \left[\frac{k_{\perp\sigma} k_{\perp\sigma'}}{k_\perp^2} - \frac{g_{\perp\sigma\sigma'}}{2-2\epsilon} \right] \right\} \mathcal{A}_c^\sigma(t) \mathcal{A}_c^{*\sigma'}(t) . \end{aligned} \quad (\text{C.1})$$

Here again we can recognize the Altarelli-Parisi kernel for $g \rightarrow q\bar{q}$ splitting.

As done before for eq. (B.9), we can specify this formula to the problem we are studying. With the same substitutions made to go from eq. (B.9) to eq. (B.10), we can write

$$\begin{aligned} \mathcal{M}_{q\bar{q}}^{\text{col}} = & g_s^2 \mu^{2\epsilon} \frac{4 T_F}{q^2 y} \left\{ -\frac{1}{2-2\epsilon} \left[v^2 + (1-v)^2 - \epsilon \right] g_{\sigma\sigma'} \right. \\ & \left. + 2v(1-v) \left[\frac{k_{\perp\sigma} k_{\perp\sigma'}}{k_\perp^2} - \frac{g_{\perp\sigma\sigma'}}{2-2\epsilon} \right] \right\} \times \mathcal{M}_b^{\sigma\sigma'} . \end{aligned} \quad (\text{C.2})$$

Appendix D: Soft limit for the invariant amplitude $Q\bar{Q}gg$

In this appendix we will derive the divergent part of the invariant amplitude for the process

$$Z/\gamma(q) \rightarrow Q(p) + \bar{Q}(p') + g(k) + g(l) \quad (\text{D.1})$$

in the limit when the momentum l of the gluon is soft. A soft singularity appears only if the soft gluon is emitted from one of the external legs. If the emitting external particle is the gluon, the amplitude of the process, in the Feynman gauge, is

$$\mathcal{A}_{ij}^{ab(\text{g})} = \mathcal{A}_{ij}^{c\sigma}(l+k) \frac{-i}{(k+l)^2} (-g_s) f^{abc} \Gamma_\sigma^{\mu\nu}(-k, -l, k+l) \epsilon_\mu(k) \bar{\epsilon}_\nu(l) ,$$

where we have added to eq. (B.1) the colour indices i, j of the produced quarks. As l goes to zero, this term develops a singularity. By using the gauge condition $k^\sigma \mathcal{A}_{c\sigma}^{ij}(k) = 0$ and the transversality $k^\mu \epsilon_\mu(k) = 0$, we can write the amplitude as

$$\mathcal{A}_{ij}^{ab(\text{g})} = g_s f^{abc} \frac{k^\nu}{k \cdot l} \mathcal{A}_{ij}^{c\sigma}(k) \epsilon_\sigma(k) \bar{\epsilon}_\nu(l) + \text{non-singular terms.} \quad (\text{D.2})$$

Similarly, if we consider the emission of a soft gluon of colour index b from an external quark leg with momentum p and colour index i , that is

$$Q_n(p+l) \rightarrow Q_i(p) + g_b(l) ,$$

we can write the invariant amplitude

$$\mathcal{A}_{ij}^{ab(\text{Q})} = \bar{u}(p) (-i g_s \gamma^\nu t_{in}^b) \frac{i}{\not{p} + \not{l} - m} \tilde{\mathcal{A}}_{nj}^{a\mu}(p+l) \epsilon_\mu(k) \bar{\epsilon}_\nu(l) ,$$

where $\tilde{\mathcal{A}}$ refers to the rest of the process from which the quark external line takes origin.

In the limit of l going to zero, we can rewrite this amplitude as

$$\mathcal{A}_{ij}^{ab(\text{Q})} = g_s \frac{p^\nu}{p \cdot l} t_{in}^b \mathcal{A}_{nj}^{a\mu}(p) \epsilon_\mu(k) \bar{\epsilon}_\nu(l) + \text{non-singular terms,} \quad (\text{D.3})$$

where we have defined $\mathcal{A}_{nj}^{a\mu}(p) = \bar{u}(p) \tilde{\mathcal{A}}_{nj}^{a\mu}(p)$.

In the same way, we can obtain the limit of the amplitude for the soft emission from an antiquark with momentum p' and colour index j

$$\mathcal{A}_{ij}^{ab(\bar{Q})} = -g_s \frac{p'^\nu}{p' \cdot l} \mathcal{A}_{in}^{a\mu}(p') t_{nj}^b \epsilon_\mu(k) \bar{\epsilon}_\nu(l) + \text{non-singular terms.} \quad (\text{D.4})$$

Considering that $\mathcal{A}_{ij}^{c\sigma} = t_{ij}^c \mathcal{A}^\sigma$, where \mathcal{A}^σ does not contain any colour element, and the similar ones for eqs. (D.3) and (D.4), we can sum the three amplitudes to obtain

$$\mathcal{A}_{ij}^{ab} = g_s \left\{ i f^{abc} \frac{k^\nu}{k \cdot l} t_{ij}^c + \frac{p^\nu}{p \cdot l} t_{in}^b t_{nj}^a - \frac{p''^\nu}{p' \cdot l} t_{in}^a t_{nj}^b \right\} \mathcal{A}^\mu \epsilon_\mu(k) \bar{\epsilon}_\nu(l)$$

where we have disregarded the non-singular terms.

By squaring the amplitude and summing over the spins and colours of the final gluons and quarks, we have

$$\begin{aligned} \mathcal{M}_{gg}^{\text{soft}}(l) = g_s^2 \mu^{2\epsilon} & \left\{ -C_A \left[\frac{p \cdot k}{(p \cdot l)(k \cdot l)} + \frac{p' \cdot k}{(p' \cdot l)(k \cdot l)} \right] + \right. \\ & \left. - 2 \left(C_F - \frac{C_A}{2} \right) \frac{p \cdot p'}{(p \cdot l)(p' \cdot l)} + C_F \left[\frac{m^2}{(p \cdot l)^2} + \frac{m^2}{(p' \cdot l)^2} \right] \right\} \times \mathcal{M}_\sigma^\sigma \end{aligned} \quad (\text{D.5})$$

where we have made use of eq. (4.16).

The same result applies in the case of k soft, once the interchange $l \leftrightarrow k$ is made.

Appendix E: One-loop scalar integrals

We can classify the different types of scalar integrals according to the number of massive propagators in the loop and according to the “shape” of the loop: boxes (B) and triangles (T). We introduce the following kinematical invariants

$$\begin{aligned} \sigma_1 &= (q - p')^2 - m^2 = q^2(1 - x_2) \\ \sigma_2 &= (q - p)^2 - m^2 = q^2(1 - x_1) \\ \sigma_3 &= (q - k)^2 = q^2(1 - x_g) , \end{aligned} \quad (\text{E.1})$$

where x_1 and x_2 are defined by (3.8) and x_g by (3.11), and

$$\lambda_\pm = \frac{1}{2} \left(1 \pm \sqrt{1 - \frac{4m^2}{q^2}} \right) \equiv \frac{1}{2} (1 \pm \Delta)$$

$$\xi_\pm = \frac{1}{2} \left(1 \pm \sqrt{1 - \frac{4m^2}{\sigma_3}} \right) \equiv \frac{1}{2} (1 \pm \Delta')$$

$$\rho_\pm = \frac{1}{2} \left[\alpha_1 \pm \sqrt{\alpha_1^2 - \frac{4m^2}{q^2}} \right] \quad \text{with: } \alpha_1 = 1 - \frac{\sigma_1}{q^2}$$

$$\eta_{\pm} = \frac{1}{2} (\Delta' \pm \Delta) .$$

Here we also give the absorptive parts of the integrals, although they do not contribute to the cross section. The integrals are computed in $d = 4 - 2\epsilon$ dimensions. Terms of order ϵ or higher have been dropped.

Defining the dilogarithm function as

$$\text{Li}_2(x) = - \int_0^x dz \frac{\log(1-z)}{z}$$

and collecting the same factor

$$N(\epsilon) = \frac{i}{16\pi^2} (4\pi)^\epsilon \Gamma(1+\epsilon) = i N_\epsilon$$

in front of each expression, we obtain

$$\begin{aligned} B_{2m} &\equiv \int \frac{d^d l}{(2\pi)^d} \frac{1}{l^2} \frac{1}{(l-k)^2} \frac{1}{(l+p-q)^2 - m^2} \frac{1}{(l+p)^2 - m^2} \\ &= N(\epsilon) (m^2)^{-\epsilon} \frac{1}{\sigma_1 \sigma_2} \left\{ \frac{1}{\epsilon^2} + \frac{1}{\epsilon} \left(\log \frac{m^2}{\sigma_1} + \log \frac{m^2}{\sigma_2} \right) + 2 \log \frac{m^2}{\sigma_1} \log \frac{m^2}{\sigma_2} \right. \\ &\quad \left. - \frac{5}{3} \pi^2 - \log^2 \frac{\lambda_+}{\lambda_-} + 2\pi i \left[\frac{1}{\epsilon} + \log \frac{m^2}{\sigma_1} + \log \frac{m^2}{\sigma_2} + \log \frac{\lambda_+}{\lambda_-} \right] \right\} \end{aligned} \quad (\text{E.2})$$

$$\begin{aligned} B_{3m} &\equiv \int \frac{d^d l}{(2\pi)^d} \frac{1}{l^2} \frac{1}{(l+p)^2 - m^2} \frac{1}{(l+p-q)^2 - m^2} \frac{1}{(l-p')^2 - m^2} \\ &= N(\epsilon) (m^2)^{-\epsilon} \frac{1}{\sigma_2 \sigma_3 \Delta'} \left\{ \frac{1}{\epsilon} \log \frac{\xi_-}{\xi_+} + \left(2 \log \frac{m^2}{\sigma_2} + \log \frac{m^2}{\sigma_3} \right) \log \frac{\xi_-}{\xi_+} \right. \\ &\quad - 2 \text{Li}_2(\xi_-) - \log^2 \xi_- - 2 \text{Li}_2\left(-\frac{\lambda_-}{\eta_+}\right) - 2 \text{Li}_2\left(\frac{\eta_+}{\lambda_+}\right) - \log^2 \frac{\lambda_+}{\eta_+} \\ &\quad + 2 \text{Li}_2\left(\frac{\lambda_-}{\eta_-}\right) + 2 \text{Li}_2\left(-\frac{\eta_-}{\lambda_+}\right) + \log^2 \left(-\frac{\lambda_+}{\eta_-}\right) + 2 \text{Li}_2\left(-\frac{\xi_-}{\Delta'}\right) - \frac{\pi^2}{2} \\ &\quad + 2 \log \left(-\frac{\eta_+}{\eta_-}\right) \log \frac{\lambda_-}{\lambda_+} + \log^2 \xi_+ - 2 \log \Delta' \log \xi_- + \log^2 \Delta' \\ &\quad \left. + i\pi \left[\frac{1}{\epsilon} + 2 \log \frac{q^2}{\sigma_2} + 4 \log \eta_+ - 2 \log \Delta' + 2 \log \frac{\xi_-}{\xi_+} \right] \right\} \end{aligned} \quad (\text{E.3})$$

$$T_{2m}^q \equiv \int \frac{d^d l}{(2\pi)^d} \frac{1}{l^2} \frac{1}{(l-p')^2 - m^2} \frac{1}{(l+p+k)^2 - m^2}$$

$$\begin{aligned}
&= N(\epsilon) (m^2)^{-\epsilon} \frac{-1}{q^2 \sqrt{\alpha_1^2 - \frac{4m^2}{q^2}}} \left\{ \text{Li}_2 \left(1 - \frac{1}{\rho_+} \right) + \text{Li}_2 \left(-\frac{\rho_+}{\lambda_+ - \rho_+} \right) \right. \\
&\quad + \text{Li}_2 \left(\frac{\lambda_+ - \rho_+}{1 - \rho_+} \right) - \text{Li}_2 \left(\frac{\rho_+ - \lambda_-}{\rho_+} \right) - \text{Li}_2 \left(\frac{1 - \rho_+}{\lambda_- - \rho_+} \right) - \text{Li}_2 (\rho_-) \\
&\quad - \text{Li}_2 \left(\frac{\lambda_+ - \rho_-}{1 - \rho_-} \right) - \text{Li}_2 \left(-\frac{\rho_-}{\lambda_+ - \rho_-} \right) + \text{Li}_2 \left(\frac{\lambda_-}{\lambda_- - \rho_-} \right) \\
&\quad + \text{Li}_2 \left(\frac{\rho_- - \lambda_-}{1 - \lambda_-} \right) + \frac{1}{2} \log^2 \frac{\lambda_+ - \rho_+}{1 - \rho_+} - \frac{1}{2} \log^2 \frac{\rho_+ - \lambda_-}{\rho_+} - \frac{1}{2} \log^2 \rho_- \\
&\quad - \log \rho_- \log \frac{1 - \rho_-}{\rho_-} - \frac{1}{2} \log^2 \frac{\lambda_+ - \rho_-}{1 - \rho_-} + \frac{1}{2} \log^2 \frac{\rho_- - \lambda_-}{1 - \lambda_-} \\
&\quad - \log \frac{\rho_- - 1}{\lambda_- - \rho_-} \log \frac{\lambda_- - 1}{\lambda_- - \rho_-} + \log \frac{-\rho_-}{\lambda_- - \rho_-} \log \frac{-\lambda_-}{\lambda_- - \rho_-} + \frac{\pi^2}{6} \\
&\quad \left. + i\pi \left[2 \log \frac{\lambda_+ - \rho_-}{\lambda_+ - \rho_+} + \log \frac{1 - \rho_+}{1 - \rho_-} \right] \right\} \tag{E.4}
\end{aligned}$$

$$\begin{aligned}
T_{2m}^{q-k} &\equiv \int \frac{d^d l}{(2\pi)^d} \frac{1}{l^2} \frac{1}{(l - p')^2 - m^2} \frac{1}{(l + p)^2 - m^2} \\
&= N(\epsilon) (m^2)^{-\epsilon} \frac{1}{\sigma_3 \Delta'} \left\{ \frac{1}{\epsilon} \log \frac{\xi_-}{\xi_+} + \log \frac{m^2}{\sigma_3} \log \frac{\xi_-}{\xi_+} - \frac{1}{2} \log^2 \xi_- \right. \\
&\quad + \frac{1}{2} \log^2 \xi_+ - \log \Delta' \log \frac{\xi_-}{\xi_+} + \text{Li}_2 \left(-\frac{\xi_-}{\Delta'} \right) + \text{Li}_2 \left(\frac{\Delta'}{\xi_+} \right) + \frac{1}{2} \log^2 \frac{\xi_+}{\Delta'} \\
&\quad \left. - \frac{5}{6} \pi^2 + i\pi \left[\frac{1}{\epsilon} + \log \frac{m^2}{\sigma_3} - 2 \log \Delta' \right] \right\} \tag{E.5}
\end{aligned}$$

$$\begin{aligned}
T_{2m} &\equiv \int \frac{d^d l}{(2\pi)^d} \frac{1}{l^2} \frac{1}{(p + l)^2 - m^2} \frac{1}{(p + k + l)^2 - m^2} \\
&= N(\epsilon) (m^2)^{-\epsilon} \frac{1}{\sigma_1} \left\{ \text{Li}_2 \left(-\frac{\sigma_1}{m^2} \right) + \log \frac{\sigma_1}{m^2} \log \left(1 + \frac{\sigma_1}{m^2} \right) \right. \\
&\quad \left. - i\pi \log \left(1 + \frac{\sigma_1}{m^2} \right) \right\} \tag{E.6}
\end{aligned}$$

$$\begin{aligned}
T_{1m} &\equiv \int \frac{d^d l}{(2\pi)^d} \frac{1}{l^2} \frac{1}{(l + k)^2} \frac{1}{(l + p + k)^2 - m^2} \\
&= N(\epsilon) (m^2)^{-\epsilon} \frac{1}{\sigma_1} \left\{ \frac{1}{2\epsilon^2} + \frac{1}{\epsilon} \log \frac{m^2}{\sigma_1} + \log \frac{m^2}{\sigma_1} \log \left(1 + \frac{m^2}{\sigma_1} \right) \right\}
\end{aligned}$$

$$- \operatorname{Li}_2\left(-\frac{\sigma_1}{m^2}\right) - \frac{5}{6}\pi^2 + i\pi \left[\frac{1}{\epsilon} + \log\left(1 + \frac{\sigma_1}{m^2}\right) + 2\log\frac{m^2}{\sigma_1} \right] \quad (\text{E.7})$$

$$\begin{aligned} T_{3m} &\equiv \int \frac{d^d l}{(2\pi)^d} \frac{1}{(l-p')^2 - m^2} \frac{1}{(l+p-q)^2 - m^2} \frac{1}{(l+p)^2 - m^2} \\ &= N(\epsilon) (m^2)^{-\epsilon} \frac{1}{2} \frac{1}{\sigma_3 - q^2} \left\{ \log^2\left(\frac{1}{\xi_-} - 1\right) - \log^2\left(\frac{1}{\lambda_-} - 1\right) \right. \\ &\quad \left. - 2i\pi \left[\log\left(\frac{1}{\xi_-} - 1\right) - \log\left(\frac{1}{\lambda_-} - 1\right) \right] \right\} \end{aligned} \quad (\text{E.8})$$

A partial check of the correctness of the above formulae can be performed in the following way. We consider first a check of B_{2m} . To this purpose, define I to be

$$\begin{aligned} I &\equiv \int \frac{d^d l}{(2\pi)^d} \frac{1 + A(l-k)^2 + B[(l+p-q)^2 - m^2] + C[(l+p)^2 - m^2]}{l^2(l-k)^2 [(l+p-q)^2 - m^2] [(l+p)^2 - m^2]} = \\ &= \int \frac{d^d l}{(2\pi)^d} \frac{1 + B[q^2 - 2p \cdot q] + 2l \cdot [-Ak + B(p-q) + Cp] + l^2(A + B + C)}{l^2(l-k)^2 [(l+p-q)^2 - m^2] [(l+p)^2 - m^2]} \end{aligned}$$

If we impose that I has no infrared and collinear divergences, then

$$\begin{cases} 1 + B[q^2 - 2p \cdot q] = 0 \\ k \cdot [-Ak + B(p-q) + Cp] = 0 \end{cases}$$

Solving this system

$$\begin{cases} B = -\frac{1}{\sigma_2} \\ C = -\frac{1}{\sigma_1} \end{cases}$$

So I can be rewritten as

$$I = B_{2m} + AT_{2m}'^q - \frac{1}{\sigma_2} T_{1m} - \frac{1}{\sigma_1} T_{1m}'$$

where the primed quantities are the same as before, with the substitution $p \leftrightarrow p'$, that is $\sigma_1 \leftrightarrow \sigma_2$. The integral I is now convergent and the cancellation of the divergent part of the right-hand side can be checked directly (both in the real part and in the absorptive one). As far as the finite terms are concerned, the integral I can be reduced to a one-variable integral, using Feynman parametrization, and then integrated numerically to check the identity.

With the same reasoning, we can check B_{3m} . We introduce the integral

$$I \equiv \int \frac{d^d l}{(2\pi)^d} \frac{1 + A [(l+p)^2 - m^2] + B [(l+p-q)^2 - m^2] + C [(l-p')^2 - m^2]}{l^2 [(l+p)^2 - m^2] [(l+p-q)^2 - m^2] [(l-p')^2 - m^2]} \\ = \int \frac{d^d l}{(2\pi)^d} \frac{1 + B [q^2 - 2p \cdot q] + 2l \cdot [Ap + B(p-q) - Cp'] + l^2(A + B + C)}{l^2 [(l+p)^2 - m^2] [(l+p-q)^2 - m^2] [(l-p')^2 - m^2]}.$$

This integral has only soft divergences, which can be removed if we require that

$$1 + B [q^2 - 2p \cdot q] = 0 \implies B = -\frac{1}{\sigma_2}.$$

Thus I becomes

$$I = B_{3m} + AT'_{2m} - \frac{1}{\sigma_2} T_{2m}^{q-k} + CT_{2m}^{'q}.$$

The rest of the check is the same as before.

Appendix F: List of integrals for the soft contributions

We now summarize the values of the integrals required to isolate the singular pieces of the four-jet cross section, in the soft-gluon limit

$$I_1(x, h) = \int_0^x dy \int_0^1 dv [v(1-v)]^{-\epsilon} y^{-\epsilon} \frac{1}{y[y+hv]} = \\ = \frac{1}{2h} \left\{ \frac{1}{\epsilon^2} - \frac{1}{\epsilon} \log h - \log^2 \frac{x}{h} + \frac{1}{2} \log^2 h - \frac{\pi^2}{2} - 2 \text{Li}_2 \left(-\frac{x}{h} \right) \right\} + \mathcal{O}(\epsilon)$$

$$I_2(x, h) = \int_0^x dy \int_0^1 dv [v(1-v)]^{-\epsilon} y^{-\epsilon} \frac{1}{[y+hv]^2} = \\ = \frac{1}{2h} \left\{ -\frac{1}{\epsilon} - 2 \log \left(1 + \frac{h}{x} \right) + \log h \right\} + \mathcal{O}(\epsilon)$$

$$I_3 = \frac{1}{N_\phi} \int_0^\pi d\phi (\sin \phi)^{-2\epsilon} \int_0^x dy \int_0^1 dv [v(1-v)]^{-\epsilon} y^{-\epsilon} \\ \times \frac{1}{y+hv} \frac{1}{y - c \cos \phi \sqrt{y} \sqrt{v+gv}} = \\ = \frac{1}{N_\phi} \left\{ -\frac{1}{2\epsilon} I_\epsilon + I_\phi - \frac{1}{2} [-I_x + I_{1/x}] \right\} + \mathcal{O}(\epsilon)$$

where I_ϵ, I_ϕ, I_x and $I_{1/x}$ are finite quantities, defined by

$$\begin{aligned}
 I_\epsilon &= \frac{\pi}{K} \frac{(1 + \Delta'^2)(1 - \Delta'^2)}{4\Delta'} (1 - x_g) \log \left(\frac{\xi_+}{\xi_-} \right)^2 \\
 I_\phi &= \int_0^{\frac{\pi}{2}} d\phi \log \sin \phi \frac{2}{(g - h)^2 + h(c \cos \phi)^2} \\
 &\quad \times \left\{ \frac{2c(g + h) \cos \phi}{\sqrt{4g - c^2 \cos^2 \phi}} \arctan \frac{c \cos \phi}{\sqrt{4g - c^2 \cos^2 \phi}} + (g - h) \log \frac{g}{h} \right\} \\
 I_x &= \int_0^x dt \frac{\log t}{(h + t)} \frac{\pi}{\sqrt{(t + g)^2 - c^2 t}} \\
 I_{1/x} &= \int_0^{\frac{1}{x}} dt \frac{-2 \log x - \log t}{(1 + ht)} \frac{\pi}{\sqrt{(1 + gt)^2 - c^2 t}}.
 \end{aligned}$$

For the definition of the constants appearing in these integrals, see Section 4.4 and Appendix E.

Appendix G: Results

We implemented our analytical result in a FORTRAN program, which behaves like a “partonic” Monte Carlo generator, analogous to the program EVENT [9]. We collect here some results obtained with our code, with which future users of the program may, eventually, compare their results. Furthermore, since for this kind of calculations it would be difficult to perform analytical comparisons, the only possible alternative is to choose a few shape variables, and compare numerical results, in the spirit of what has been done in ref. [17] for the case of the massless calculation.

We include in these results only the contributions from cut graphs of A-type, that is to say, from cut graphs in which the weak current couples to the same heavy-flavour loop, and there is a single $Q\bar{Q}$ pair in the final state, which is the really hard part of the calculation. For the contributions involving two heavy-quark pairs in the final state, it is easier to compare directly the value of the matrix elements squared (this part of our program was in fact checked in this way with the program of ref. [10]).

We have chosen a set of shape variables for which it should be easy to obtain quite accurate numerical results. We have fixed the centre-of-mass energy to be 100 GeV, and the mass of the heavy quark has been taken to be equal to 1, 10, 20 and 30 GeV. We present separately the results for a hypothetical vector boson with purely axial or purely vector couplings, normalized to the massless total cross section at the zeroth order in α_s . We have chosen the following shape variables: the thrust t , the c parameter, the mass of the heavy jet squared M_h^2 (according to the thrust axis), the energy–energy correlation EEC, the three-jet fractions according to the E, EM, JADE, and DURHAM schemes. For t , c , M_h^2 and EEC we present moments, instead of distributions, because they can be obtained with higher precision. For thrust, for example, we thus compute, according to the notation of Section 4

$$\int dT_{V/A} (1-t)^n = \left(\frac{\alpha_s}{2\pi}\right) A_{V/A}^t(n) + \left(\frac{\alpha_s}{2\pi}\right)^2 B_{V/A}^t(n) . \quad (\text{G.1})$$

We will further decompose

$$B_{V/A}^t = B_{V/A, C_A}^t + B_{V/A, C_F}^t + B_{V/A, T_F}^t , \quad (\text{G.2})$$

where the C_A , C_F and T_F subscripts denote the $C_F C_A$, C_F^2 and $n_f C_F T_F$ colour components. For some shape variables, the presence of massive particles in the final state may introduce ambiguities in the definition, owing to the fact that, in the massless case, energy and momentum can be interchanged. We thus refer to the exact definitions given in ref. [9] for t , c , M_h^2 and in ref. [17] for the EEC. Moments are defined as

$$\begin{aligned} \int dT_{V/A} c^n &= \left(\frac{\alpha_s}{2\pi}\right) A_{V/A}^c(n) + \left(\frac{\alpha_s}{2\pi}\right)^2 B_{V/A}^c(n) , \\ \int dT_{V/A} \left(\frac{M_h^2 - m^2}{q^2}\right)^n &= \left(\frac{\alpha_s}{2\pi}\right) A_{V/A}^{M_h}(n) + \left(\frac{\alpha_s}{2\pi}\right)^2 B_{V/A}^{M_h}(n) , \\ \int dT_{V/A} \sum_{ij} \frac{E_i E_j}{q^2} \cos^k \theta_{ij} \sin^{2+n} \theta_{ij} &= \left(\frac{\alpha_s}{2\pi}\right) A_{V/A}^{\text{EEC}}(n, k) + \left(\frac{\alpha_s}{2\pi}\right)^2 B_{V/A}^{\text{EEC}}(n, k) . \end{aligned}$$

where the sum runs over all the final particles.

Clusters are defined in the following way. There is a resolution parameter y , which is computed for every pair of particles in the final state. One finds the pair for which y is minimum. If $y < y_{cut}$ the two particles are combined into a single pseudo-particle by adding up their four momenta. One thus computes

$$\int dT_{V/A} \delta_{N_X(y_{cut}), 3} = \left(\frac{\alpha_s}{2\pi}\right) A_{V/A}^X(y_{cut}) + \left(\frac{\alpha_s}{2\pi}\right)^2 B_{V/A}^X(y_{cut}) , \quad (\text{G.3})$$

where X stands for E, EM, JADE or DURHAM, and $N_X(y_{cut})$ is the number of pseudo-particles in the final state after the clustering procedure. The various clustering algorithms differ by the definition of the resolution parameter y

$$\begin{aligned}
 \text{E} &: \frac{(p_i + p_j)^2}{q^2} , \\
 \text{EM} &: 2 \frac{p_i \cdot p_j}{q^2} , \\
 \text{JADE} &: 2 \frac{E_i E_j}{q^2} (1 - \cos \theta_{ij}) , \\
 \text{DURHAM} &: 2 \min(E_i^2, E_j^2) \frac{1}{q^2} (1 - \cos \theta_{ij}) . \tag{G.4}
 \end{aligned}$$

Observe that the E scheme is not infrared-safe if $y_{cut} < m^2/q^2$. In fact, in this case, the configuration made up of two heavy quarks plus a soft gluon cannot be reduced to two pseudo-particles, since the recombination parameter will fail the cut, for any pair containing a massive quark. The cancellation of soft divergences cannot therefore work for these values of the cut parameter.

We have chosen the renormalization scale $\mu = E$, and $n_f = 5$. The results are given in Tables 1 to 9.

n	$m/E = 0.01$	$m/E = 0.1$	$m/E = 0.2$	$m/E = 0.3$
$B_{V, C_A}^t(n)$				
1	71.53 ± 0.045	57.14 ± 0.024	39.17 ± 0.013	21.83 ± 0.006
2	5.303 ± 0.005	4.47 ± 0.0034	3.026 ± 0.002	$1.524 \pm 8 \cdot 10^{-4}$
3	0.8056 ± 0.0012	$0.6887 \pm 8 \cdot 10^{-4}$	$0.4582 \pm 5 \cdot 10^{-4}$	$0.2127 \pm 2 \cdot 10^{-4}$
4	$0.1604 \pm 3.4 \cdot 10^{-4}$	$0.1381 \pm 2.4 \cdot 10^{-4}$	$0.09096 \pm 1.4 \cdot 10^{-4}$	$0.04003 \pm 6 \cdot 10^{-5}$
5	$0.03668 \pm 1 \cdot 10^{-4}$	$0.03174 \pm 7 \cdot 10^{-5}$	$0.02079 \pm 4 \cdot 10^{-5}$	$0.008845 \pm 2 \cdot 10^{-5}$
$B_{V, C_F}^t(n)$				
1	-4.34 ± 0.06	-0.704 ± 0.026	2.449 ± 0.01	3.929 ± 0.003
2	2.48 ± 0.007	1.78 ± 0.004	1.127 ± 0.0014	$0.699 \pm 5 \cdot 10^{-4}$
3	0.5348 ± 0.002	0.3883 ± 0.001	$0.2316 \pm 4 \cdot 10^{-4}$	$0.1293 \pm 1.2 \cdot 10^{-4}$
4	$0.1241 \pm 6 \cdot 10^{-4}$	$0.09007 \pm 2.7 \cdot 10^{-4}$	$0.0519 \pm 1.1 \cdot 10^{-4}$	$0.02743 \pm 3.4 \cdot 10^{-5}$
5	$0.03116 \pm 1.8 \cdot 10^{-4}$	$0.02255 \pm 8 \cdot 10^{-5}$	$0.01261 \pm 3.5 \cdot 10^{-5}$	$0.006392 \pm 1 \cdot 10^{-5}$
$B_{V, T_F}^t(n)$				
1	-22.37 ± 0.004	-18.48 ± 0.005	-13.17 ± 0.004	-7.767 ± 0.002
2	$-1.552 \pm 6 \cdot 10^{-4}$	$-1.38 \pm 7 \cdot 10^{-4}$	$-1.017 \pm 5 \cdot 10^{-4}$	$-0.5844 \pm 3 \cdot 10^{-4}$
3	$-0.2153 \pm 1.3 \cdot 10^{-4}$	$-0.1958 \pm 1.7 \cdot 10^{-4}$	$-0.1465 \pm 1.2 \cdot 10^{-4}$	$-0.08272 \pm 7 \cdot 10^{-5}$
4	$-0.03864 \pm 3.5 \cdot 10^{-5}$	$-0.03559 \pm 4 \cdot 10^{-5}$	$-0.027 \pm 3 \cdot 10^{-5}$	$-0.01515 \pm 1.8 \cdot 10^{-5}$
5	$-0.007897 \pm 1 \cdot 10^{-5}$	$-0.007344 \pm 1.3 \cdot 10^{-5}$	$-0.005647 \pm 9 \cdot 10^{-6}$	$-0.003174 \pm 5 \cdot 10^{-6}$
$B_{A, C_A}^t(n)$				
1	71.5 ± 0.045	54.27 ± 0.023	31.33 ± 0.01	12.46 ± 0.0035
2	5.301 ± 0.005	4.284 ± 0.003	2.501 ± 0.0015	$0.9336 \pm 5 \cdot 10^{-4}$
3	0.8054 ± 0.0012	$0.6637 \pm 8 \cdot 10^{-4}$	$0.3874 \pm 4 \cdot 10^{-4}$	$0.138 \pm 1.2 \cdot 10^{-4}$
4	$0.1603 \pm 3.4 \cdot 10^{-4}$	$0.1336 \pm 2.3 \cdot 10^{-4}$	$0.07807 \pm 1 \cdot 10^{-4}$	$0.02708 \pm 3.6 \cdot 10^{-5}$
5	$0.03667 \pm 1 \cdot 10^{-4}$	$0.03077 \pm 7 \cdot 10^{-5}$	$0.01802 \pm 3.5 \cdot 10^{-5}$	$0.006162 \pm 1.1 \cdot 10^{-5}$
$B_{A, C_F}^t(n)$				
1	-4.3 ± 0.06	0.5 ± 0.025	3.942 ± 0.008	3.722 ± 0.002
2	2.481 ± 0.007	1.801 ± 0.0036	1.109 ± 0.0012	$0.5694 \pm 3 \cdot 10^{-4}$
3	0.535 ± 0.002	$0.3871 \pm 9 \cdot 10^{-4}$	$0.221 \pm 3 \cdot 10^{-4}$	$0.1041 \pm 8 \cdot 10^{-5}$
4	$0.1241 \pm 6 \cdot 10^{-4}$	$0.0893 \pm 2.6 \cdot 10^{-4}$	$0.04897 \pm 9 \cdot 10^{-5}$	$0.02206 \pm 2 \cdot 10^{-5}$
5	$0.03116 \pm 1.8 \cdot 10^{-4}$	$0.02228 \pm 8 \cdot 10^{-5}$	$0.01181 \pm 3 \cdot 10^{-5}$	$0.005136 \pm 7 \cdot 10^{-6}$
$B_{A, T_F}^t(n)$				
1	-22.36 ± 0.004	-17.5 ± 0.005	-10.49 ± 0.003	-4.457 ± 0.0013
2	$-1.552 \pm 6 \cdot 10^{-4}$	$-1.311 \pm 7 \cdot 10^{-4}$	$-0.8247 \pm 4 \cdot 10^{-4}$	$-0.3533 \pm 1.7 \cdot 10^{-4}$
3	$-0.2152 \pm 1.3 \cdot 10^{-4}$	$-0.1861 \pm 1.6 \cdot 10^{-4}$	$-0.1197 \pm 9 \cdot 10^{-5}$	$-0.05156 \pm 4 \cdot 10^{-5}$
4	$-0.03862 \pm 3.5 \cdot 10^{-5}$	$-0.03382 \pm 4 \cdot 10^{-5}$	$-0.0221 \pm 2.5 \cdot 10^{-5}$	$-0.009594 \pm 1 \cdot 10^{-5}$
5	$-0.007893 \pm 1 \cdot 10^{-5}$	$-0.00697 \pm 1.2 \cdot 10^{-5}$	$-0.004616 \pm 7 \cdot 10^{-6}$	$-0.002024 \pm 3 \cdot 10^{-6}$

Table 1: The thrust t .

n	$m/E = 0.01$	$m/E = 0.1$	$m/E = 0.2$	$m/E = 0.3$
$B_{V, C_A}^{M_h}(n)$				
1	68.32 ± 0.05	56.71 ± 0.03	38.45 ± 0.02	19.46 ± 0.008
2	4.591 ± 0.006	4.014 ± 0.004	2.642 ± 0.0035	1.029 ± 0.0024
3	0.6336 ± 0.0013	0.5549 ± 0.001	0.3565 ± 0.0013	0.1072 ± 0.001
4	$0.1156 \pm 3.6 \cdot 10^{-4}$	$0.1002 \pm 3 \cdot 10^{-4}$	$0.0641 \pm 5 \cdot 10^{-4}$	$0.0167 \pm 4.5 \cdot 10^{-4}$
5	$0.02447 \pm 1 \cdot 10^{-4}$	$0.02084 \pm 1 \cdot 10^{-4}$	$0.01346 \pm 1.8 \cdot 10^{-4}$	$0.0037 \pm 2 \cdot 10^{-4}$
$B_{V, C_F}^{M_h}(n)$				
1	-21.39 ± 0.05	-10.55 ± 0.026	-1.143 ± 0.01	3.166 ± 0.004
2	0.218 ± 0.007	0.4605 ± 0.004	0.7282 ± 0.002	0.736 ± 0.0011
3	0.0784 ± 0.002	0.119 ± 0.001	$0.162 \pm 6 \cdot 10^{-4}$	$0.1834 \pm 5 \cdot 10^{-4}$
4	$0.0165 \pm 6 \cdot 10^{-4}$	$0.02626 \pm 3 \cdot 10^{-4}$	$0.03773 \pm 2 \cdot 10^{-4}$	$0.055 \pm 2 \cdot 10^{-4}$
5	$0.00365 \pm 1.8 \cdot 10^{-4}$	$0.00619 \pm 1 \cdot 10^{-4}$	$0.00959 \pm 8 \cdot 10^{-5}$	$0.01829 \pm 9 \cdot 10^{-5}$
$B_{V, T_F}^{M_h}(n)$				
1	-23.2 ± 0.005	-20.04 ± 0.006	-14.32 ± 0.004	-7.809 ± 0.0025
2	$-1.704 \pm 6 \cdot 10^{-4}$	$-1.563 \pm 8 \cdot 10^{-4}$	$-1.153 \pm 7 \cdot 10^{-4}$	$-0.5961 \pm 5 \cdot 10^{-4}$
3	$-0.2505 \pm 1.4 \cdot 10^{-4}$	$-0.2308 \pm 2 \cdot 10^{-4}$	$-0.1753 \pm 2 \cdot 10^{-4}$	$-0.1014 \pm 2 \cdot 10^{-4}$
4	$-0.04758 \pm 3.6 \cdot 10^{-5}$	$-0.04375 \pm 5 \cdot 10^{-5}$	$-0.03474 \pm 6 \cdot 10^{-5}$	$-0.02601 \pm 8 \cdot 10^{-5}$
5	$-0.0103 \pm 1 \cdot 10^{-5}$	$-0.009445 \pm 1.5 \cdot 10^{-5}$	$-0.007984 \pm 2 \cdot 10^{-5}$	$-0.0082 \pm 3 \cdot 10^{-5}$
$B_{A, C_A}^{M_h}(n)$				
1	68.29 ± 0.05	53.84 ± 0.03	30.76 ± 0.016	10.99 ± 0.006
2	4.59 ± 0.006	3.841 ± 0.004	2.187 ± 0.004	0.6034 ± 0.0018
3	0.6334 ± 0.0013	0.533 ± 0.001	0.3026 ± 0.0015	$0.0638 \pm 8 \cdot 10^{-4}$
4	$0.1156 \pm 3.6 \cdot 10^{-4}$	$0.0965 \pm 3 \cdot 10^{-4}$	$0.0553 \pm 6 \cdot 10^{-4}$	$0.0102 \pm 3.4 \cdot 10^{-4}$
5	$0.02447 \pm 1 \cdot 10^{-4}$	$0.02013 \pm 1 \cdot 10^{-4}$	$0.01173 \pm 2 \cdot 10^{-4}$	$0.00246 \pm 1.4 \cdot 10^{-4}$
$B_{A, C_F}^{M_h}(n)$				
1	-21.35 ± 0.05	-8.804 ± 0.025	1.276 ± 0.009	3.617 ± 0.0026
2	0.22 ± 0.007	0.546 ± 0.004	0.8205 ± 0.0017	$0.7156 \pm 7 \cdot 10^{-4}$
3	0.0787 ± 0.002	0.1304 ± 0.001	$0.1712 \pm 6 \cdot 10^{-4}$	$0.1817 \pm 3 \cdot 10^{-4}$
4	$0.0166 \pm 6 \cdot 10^{-4}$	$0.02845 \pm 3 \cdot 10^{-4}$	$0.03897 \pm 2 \cdot 10^{-4}$	$0.05504 \pm 1.2 \cdot 10^{-4}$
5	$0.00366 \pm 1.8 \cdot 10^{-4}$	$0.0067 \pm 9 \cdot 10^{-5}$	$0.00974 \pm 8 \cdot 10^{-5}$	$0.01825 \pm 5 \cdot 10^{-5}$
$B_{A, T_F}^{M_h}(n)$				
1	-23.19 ± 0.005	-19.01 ± 0.005	-11.52 ± 0.0033	-4.617 ± 0.0015
2	$-1.704 \pm 6 \cdot 10^{-4}$	$-1.491 \pm 8 \cdot 10^{-4}$	$-0.9601 \pm 6 \cdot 10^{-4}$	$-0.4038 \pm 3.6 \cdot 10^{-4}$
3	$-0.2504 \pm 1.4 \cdot 10^{-4}$	$-0.2207 \pm 1.7 \cdot 10^{-4}$	$-0.149 \pm 1.5 \cdot 10^{-4}$	$-0.07702 \pm 1.4 \cdot 10^{-4}$
4	$-0.04756 \pm 3.6 \cdot 10^{-5}$	$-0.04188 \pm 4.5 \cdot 10^{-5}$	$-0.02987 \pm 5 \cdot 10^{-5}$	$-0.02099 \pm 5 \cdot 10^{-5}$
5	$-0.0103 \pm 1 \cdot 10^{-5}$	$-0.009048 \pm 1.3 \cdot 10^{-5}$	$-0.006893 \pm 1.6 \cdot 10^{-5}$	$-0.00675 \pm 2 \cdot 10^{-5}$

Table 2: The mass of the heavy jet squared M_h^2 .

n	$m/E = 0.01$	$m/E = 0.1$	$m/E = 0.2$	$m/E = 0.3$
$B_{V, C_A}^c(n)$				
1	303.3 ± 0.18	233.9 ± 0.09	155.2 ± 0.05	84.7 ± 0.023
2	70.97 ± 0.06	58.25 ± 0.03	38.33 ± 0.018	19.18 ± 0.007
3	30.55 ± 0.03	25.56 ± 0.02	16.63 ± 0.01	7.789 ± 0.004
4	16.36 ± 0.02	13.85 ± 0.012	8.955 ± 0.007	4.008 ± 0.003
5	9.784 ± 0.012	8.341 ± 0.008	5.379 ± 0.005	2.335 ± 0.002
$B_{V, C_F}^c(n)$				
1	-36.2 ± 0.2	-13.58 ± 0.1	4.84 ± 0.04	13.41 ± 0.013
2	30.42 ± 0.07	20.29 ± 0.036	12.49 ± 0.013	7.845 ± 0.004
3	20.1 ± 0.04	13.69 ± 0.02	7.741 ± 0.008	4.23 ± 0.003
4	13.19 ± 0.025	9.04 ± 0.013	4.892 ± 0.005	2.479 ± 0.002
5	9.024 ± 0.017	6.185 ± 0.009	3.232 ± 0.004	1.543 ± 0.0013
$B_{V, T_F}^c(n)$				
1	-95.12 ± 0.016	-75.92 ± 0.02	-52.26 ± 0.015	-30.07 ± 0.009
2	-20.81 ± 0.006	-18.02 ± 0.007	-12.82 ± 0.005	-7.206 ± 0.003
3	-8.117 ± 0.003	-7.227 ± 0.004	-5.243 ± 0.003	-2.915 ± 0.0018
4	-3.859 ± 0.002	-3.495 ± 0.0027	-2.581 ± 0.002	-1.435 ± 0.0012
5	-2.007 ± 0.0013	-1.842 ± 0.0018	-1.387 ± 0.0013	$-0.7771 \pm 8 \cdot 10^{-4}$
$B_{A, C_A}^c(n)$				
1	303.2 ± 0.18	222 ± 0.09	123.9 ± 0.04	48.14 ± 0.014
2	70.95 ± 0.06	55.73 ± 0.03	31.48 ± 0.014	11.58 ± 0.0045
3	30.54 ± 0.03	24.59 ± 0.018	13.95 ± 0.008	4.942 ± 0.0027
4	16.36 ± 0.02	13.36 ± 0.01	7.62 ± 0.005	2.643 ± 0.0018
5	9.782 ± 0.012	8.071 ± 0.007	4.628 ± 0.004	1.587 ± 0.0013
$B_{A, C_F}^c(n)$				
1	-36.04 ± 0.2	-8.24 ± 0.1	11.47 ± 0.03	13.16 ± 0.008
2	30.44 ± 0.07	20.63 ± 0.034	12.45 ± 0.011	6.425 ± 0.0027
3	20.11 ± 0.04	13.64 ± 0.02	7.389 ± 0.007	3.394 ± 0.0017
4	13.19 ± 0.025	8.94 ± 0.013	4.589 ± 0.004	1.975 ± 0.001
5	9.024 ± 0.017	6.091 ± 0.009	2.998 ± 0.003	$1.223 \pm 8 \cdot 10^{-4}$
$B_{A, T_F}^c(n)$				
1	-95.07 ± 0.016	-71.88 ± 0.02	-41.59 ± 0.012	-17.2 ± 0.005
2	-20.8 ± 0.006	-17.11 ± 0.007	-10.36 ± 0.004	-4.312 ± 0.0017
3	-8.113 ± 0.003	-6.865 ± 0.004	-4.263 ± 0.0025	-1.788 ± 0.001
4	-3.857 ± 0.002	-3.317 ± 0.0025	-2.099 ± 0.0016	$-0.8903 \pm 7 \cdot 10^{-4}$
5	-2.006 ± 0.0013	-1.745 ± 0.0017	-1.124 ± 0.001	$-0.4836 \pm 4.5 \cdot 10^{-4}$

Table 3: The c parameter.

n	$m/E = 0.01$	$m/E = 0.1$	$m/E = 0.2$	$m/E = 0.3$
$B_{V, C_A}^{\text{EEC}}(n, 0)$				
0	202.3 ± 0.12	154.4 ± 0.06	97.08 ± 0.03	46.81 ± 0.013
1	143.1 ± 0.1	117 ± 0.05	77.18 ± 0.026	38.2 ± 0.01
2	115.9 ± 0.09	97.55 ± 0.04	66.33 ± 0.022	33.55 ± 0.009
3	99.79 ± 0.08	85.27 ± 0.04	59.11 ± 0.02	30.38 ± 0.008
4	88.92 ± 0.08	76.65 ± 0.04	53.84 ± 0.02	28.01 ± 0.007
5	80.95 ± 0.07	70.18 ± 0.04	49.76 ± 0.018	26.13 ± 0.007
$B_{V, C_F}^{\text{EEC}}(n, 0)$				
0	-24.13 ± 0.14	-8.83 ± 0.07	3.567 ± 0.023	8.224 ± 0.007
1	-9.82 ± 0.12	-3.46 ± 0.05	3.814 ± 0.02	6.861 ± 0.006
2	-5.96 ± 0.1	-1.79 ± 0.05	3.55 ± 0.016	5.99 ± 0.005
3	-4.33 ± 0.1	-1.06 ± 0.04	3.284 ± 0.015	5.387 ± 0.005
4	-3.46 ± 0.1	-0.664 ± 0.04	3.06 ± 0.014	4.937 ± 0.0045
5	-2.92 ± 0.1	-0.43 ± 0.04	2.873 ± 0.013	4.585 ± 0.004
$B_{V, T_F}^{\text{EEC}}(n, 0)$				
0	-63.43 ± 0.01	-50.32 ± 0.014	-33.15 ± 0.009	-17.12 ± 0.005
1	-45.25 ± 0.009	-38.32 ± 0.01	-26.45 ± 0.007	-13.98 ± 0.004
2	-36.83 ± 0.008	-32.05 ± 0.01	-22.76 ± 0.006	-12.27 ± 0.0035
3	-31.8 ± 0.008	-28.07 ± 0.009	-20.3 ± 0.006	-11.11 ± 0.003
4	-28.39 ± 0.007	-25.26 ± 0.008	-18.5 ± 0.005	-10.23 ± 0.003
5	-25.88 ± 0.007	-23.15 ± 0.008	-17.1 ± 0.005	-9.544 ± 0.0027
$B_{A, C_A}^{\text{EEC}}(n, 0)$				
0	202.2 ± 0.12	146.6 ± 0.06	77.59 ± 0.027	26.66 ± 0.008
1	143 ± 0.1	111 ± 0.05	61.68 ± 0.02	21.72 ± 0.006
2	115.8 ± 0.09	92.62 ± 0.04	52.98 ± 0.018	19.05 ± 0.006
3	99.75 ± 0.08	80.96 ± 0.04	47.2 ± 0.016	17.23 ± 0.005
4	88.87 ± 0.08	72.77 ± 0.04	42.97 ± 0.015	15.87 ± 0.005
5	80.91 ± 0.07	66.62 ± 0.035	39.71 ± 0.014	14.79 ± 0.005
$B_{A, C_F}^{\text{EEC}}(n, 0)$				
0	-24.04 ± 0.14	-5.3 ± 0.06	7.765 ± 0.02	8.116 ± 0.0045
1	-9.76 ± 0.12	-0.89 ± 0.05	7.004 ± 0.016	6.709 ± 0.004
2	-5.9 ± 0.1	0.32 ± 0.045	6.252 ± 0.014	5.85 ± 0.003
3	-4.28 ± 0.1	0.78 ± 0.04	5.676 ± 0.013	5.259 ± 0.003
4	-3.41 ± 0.1	0.98 ± 0.04	5.23 ± 0.012	4.82 ± 0.003
5	-2.88 ± 0.1	1.07 ± 0.04	4.872 ± 0.011	4.476 ± 0.003
$B_{A, T_F}^{\text{EEC}}(n, 0)$				
0	-63.4 ± 0.01	-47.66 ± 0.013	-26.48 ± 0.008	-9.928 ± 0.003
1	-45.22 ± 0.009	-36.29 ± 0.01	-21.1 ± 0.006	-8.091 ± 0.0024
2	-36.81 ± 0.008	-30.35 ± 0.009	-18.15 ± 0.005	-7.085 ± 0.002
3	-31.79 ± 0.008	-26.57 ± 0.008	-16.18 ± 0.005	-6.401 ± 0.002
4	-28.38 ± 0.007	-23.91 ± 0.008	-14.73 ± 0.004	-5.889 ± 0.0017
5	-25.87 ± 0.007	-21.91 ± 0.007	-13.61 ± 0.004	-5.486 ± 0.0016

Table 4: The energy-energy correlation EEC, $k = 0$

n	$m/E = 0.01$	$m/E = 0.1$	$m/E = 0.2$	$m/E = 0.3$
$B_{V, C_A}^{\text{EEC}}(n, 1)$				
0	-26.06 ± 0.025	-21.45 ± 0.014	-14.12 ± 0.008	-7.006 ± 0.003
1	-9.56 ± 0.016	-8.967 ± 0.01	-6.413 ± 0.006	-3.152 ± 0.0023
2	-4.827 ± 0.013	-4.892 ± 0.008	-3.785 ± 0.0045	-1.898 ± 0.002
3	-2.894 ± 0.011	-3.086 ± 0.008	-2.549 ± 0.004	-1.316 ± 0.0017
4	-1.93 ± 0.01	-2.133 ± 0.007	-1.858 ± 0.0036	-0.9876 ± 0.0015
5	-1.38 ± 0.01	-1.57 ± 0.007	-1.427 ± 0.0034	-0.779 ± 0.0014
$B_{V, C_F}^{\text{EEC}}(n, 1)$				
0	8.73 ± 0.03	3.607 ± 0.015	-0.625 ± 0.006	-2.075 ± 0.002
1	0.593 ± 0.02	0.272 ± 0.01	-0.944 ± 0.004	-1.345 ± 0.0014
2	-0.588 ± 0.02	-0.327 ± 0.009	-0.786 ± 0.0034	-0.9457 ± 0.0012
3	-0.76 ± 0.018	-0.441 ± 0.008	-0.6335 ± 0.003	-0.7102 ± 0.001
4	-0.73 ± 0.017	-0.437 ± 0.007	-0.5177 ± 0.003	$-0.5588 \pm 9 \cdot 10^{-4}$
5	-0.66 ± 0.016	-0.403 ± 0.007	-0.431 ± 0.0026	$-0.4546 \pm 8 \cdot 10^{-4}$
$B_{V, T_F}^{\text{EEC}}(n, 1)$				
0	10.75 ± 0.0026	9.205 ± 0.003	6.342 ± 0.0023	3.381 ± 0.0013
1	4.47 ± 0.0018	4.256 ± 0.0023	3.179 ± 0.0016	$1.718 \pm 9 \cdot 10^{-4}$
2	2.5 ± 0.0014	2.506 ± 0.002	1.994 ± 0.0013	$1.108 \pm 7 \cdot 10^{-4}$
3	1.629 ± 0.0012	1.679 ± 0.0016	1.4 ± 0.001	$0.7997 \pm 6 \cdot 10^{-4}$
4	1.162 ± 0.001	1.218 ± 0.0014	$1.052 \pm 9 \cdot 10^{-4}$	$0.616 \pm 5 \cdot 10^{-4}$
5	0.8805 ± 0.001	0.933 ± 0.0013	$0.8273 \pm 8 \cdot 10^{-4}$	$0.4948 \pm 5 \cdot 10^{-4}$
$B_{A, C_A}^{\text{EEC}}(n, 1)$				
0	-26.05 ± 0.025	-20.4 ± 0.014	-11.39 ± 0.006	-4.12 ± 0.002
1	-9.555 ± 0.016	-8.558 ± 0.01	-5.234 ± 0.004	-1.907 ± 0.0014
2	-4.825 ± 0.013	-4.68 ± 0.008	-3.108 ± 0.0036	-1.165 ± 0.0012
3	-2.894 ± 0.011	-2.957 ± 0.007	-2.102 ± 0.003	-0.8135 ± 0.001
4	-1.93 ± 0.01	-2.047 ± 0.007	-1.535 ± 0.003	$-0.6129 \pm 9 \cdot 10^{-4}$
5	-1.38 ± 0.01	-1.508 ± 0.006	-1.182 ± 0.003	$-0.4846 \pm 9 \cdot 10^{-4}$
$B_{A, C_F}^{\text{EEC}}(n, 1)$				
0	8.71 ± 0.03	2.855 ± 0.014	-1.525 ± 0.005	-1.98 ± 0.0012
1	0.586 ± 0.02	-0.025 ± 0.01	-1.315 ± 0.0034	$-1.228 \pm 9 \cdot 10^{-4}$
2	-0.59 ± 0.02	-0.486 ± 0.008	-0.997 ± 0.003	$-0.853 \pm 7 \cdot 10^{-4}$
3	-0.763 ± 0.018	-0.541 ± 0.007	-0.7733 ± 0.0025	$-0.6373 \pm 6 \cdot 10^{-4}$
4	-0.732 ± 0.017	-0.506 ± 0.007	-0.6186 ± 0.0023	$-0.4999 \pm 6 \cdot 10^{-4}$
5	-0.66 ± 0.016	-0.454 ± 0.007	-0.508 ± 0.002	$-0.4059 \pm 5 \cdot 10^{-4}$
$B_{A, T_F}^{\text{EEC}}(n, 1)$				
0	10.75 ± 0.0026	8.765 ± 0.003	5.171 ± 0.002	$2.054 \pm 7 \cdot 10^{-4}$
1	4.468 ± 0.0018	4.06 ± 0.002	2.614 ± 0.0013	$1.07 \pm 5 \cdot 10^{-4}$
2	2.499 ± 0.0014	2.393 ± 0.0018	1.646 ± 0.001	$0.6961 \pm 4 \cdot 10^{-4}$
3	1.628 ± 0.0012	1.603 ± 0.0015	$1.157 \pm 8 \cdot 10^{-4}$	$0.5043 \pm 3.6 \cdot 10^{-4}$
4	1.162 ± 0.001	1.164 ± 0.0013	$0.8701 \pm 7 \cdot 10^{-4}$	$0.3888 \pm 3 \cdot 10^{-4}$
5	0.88 ± 0.001	0.8916 ± 0.0012	$0.6845 \pm 7 \cdot 10^{-4}$	$0.3123 \pm 3 \cdot 10^{-4}$

Table 5: The energy–energy correlation EEC, $k = 1$

y_{cut}	$m/E = 0.01$	$m/E = 0.1$	$m/E = 0.2$	$m/E = 0.3$
$B_{V, C_A}^E(y_{cut})$				
0.01	1357 ± 1.5	—	—	—
0.05	341.3 ± 0.5	374 ± 0.3	817.1 ± 0.3	—
0.10	133.7 ± 0.3	138.6 ± 0.17	164.3 ± 0.1	459.5 ± 0.17
0.15	60.75 ± 0.18	63.1 ± 0.13	64.29 ± 0.07	79.06 ± 0.04
0.20	27.13 ± 0.16	29 ± 0.12	29 ± 0.05	24.54 ± 0.027
$B_{V, C_F}^E(y_{cut})$				
0.01	-88 ± 4	—	—	—
0.05	129.8 ± 1.3	249.1 ± 0.36	0.84 ± 0.4	—
0.10	71.8 ± 0.7	120.1 ± 0.2	94.69 ± 0.07	47.95 ± 0.13
0.15	37.5 ± 0.5	53.8 ± 0.13	59.02 ± 0.045	41.25 ± 0.025
0.20	18.1 ± 0.34	24.26 ± 0.13	32.27 ± 0.03	21.58 ± 0.014
$B_{V, T_F}^E(y_{cut})$				
0.01	-452.3 ± 0.13	—	—	—
0.05	-103.8 ± 0.04	-121.3 ± 0.05	-268.6 ± 0.12	—
0.10	-38.34 ± 0.02	-42.14 ± 0.03	-54.59 ± 0.022	-154.4 ± 0.07
0.15	-16.56 ± 0.015	-17.79 ± 0.02	-21.16 ± 0.015	-28.17 ± 0.012
0.20	-6.871 ± 0.009	-7.424 ± 0.013	-8.984 ± 0.012	-9.268 ± 0.008
$B_{A, C_A}^E(y_{cut})$				
0.01	1356 ± 1.5	—	—	—
0.05	341.2 ± 0.5	355.5 ± 0.3	643 ± 0.27	—
0.10	133.6 ± 0.3	132.8 ± 0.17	133.1 ± 0.09	254.5 ± 0.09
0.15	60.9 ± 0.24	60.83 ± 0.13	53.63 ± 0.06	46.55 ± 0.03
0.20	27.1 ± 0.14	27.83 ± 0.08	25.03 ± 0.05	15.4 ± 0.016
$B_{A, C_F}^E(y_{cut})$				
0.01	-88 ± 3.6	—	—	—
0.05	130 ± 1.3	243.1 ± 0.3	32.1 ± 0.3	—
0.10	71.8 ± 0.7	117.2 ± 0.2	85.79 ± 0.06	49.67 ± 0.07
0.15	37.45 ± 0.5	52.54 ± 0.12	52.99 ± 0.04	31.7 ± 0.016
0.20	18.1 ± 0.33	23.8 ± 0.09	29.08 ± 0.03	17.24 ± 0.01
$B_{A, T_F}^E(y_{cut})$				
0.01	-452.1 ± 0.13	—	—	—
0.05	-103.8 ± 0.04	-115.4 ± 0.045	-212.6 ± 0.1	—
0.10	-38.32 ± 0.02	-40.23 ± 0.027	-44.67 ± 0.02	-86.57 ± 0.04
0.15	-16.55 ± 0.015	-17.01 ± 0.02	-17.8 ± 0.013	-17.28 ± 0.008
0.20	-6.868 ± 0.009	-7.098 ± 0.012	-7.747 ± 0.01	-6.237 ± 0.005

Table 6: The E clustering algorithm.

y_{cut}	$m/E = 0.01$	$m/E = 0.1$	$m/E = 0.2$	$m/E = 0.3$
$B_{V, C_A}^{\text{EM}}(y_{cut})$				
0.01	1340 ± 1.7	1135 ± 0.8	803.4 ± 0.4	455.7 ± 0.18
0.05	333.2 ± 0.5	291.2 ± 0.4	203.4 ± 0.18	101.6 ± 0.07
0.10	126.3 ± 0.3	111.8 ± 0.23	73.76 ± 0.11	29.24 ± 0.04
0.15	54.24 ± 0.3	48 ± 0.17	30.47 ± 0.12	8.176 ± 0.027
0.20	22.02 ± 0.2	18.85 ± 0.14	10.77 ± 0.08	1.52 ± 0.024
$B_{V, C_F}^{\text{EM}}(y_{cut})$				
0.01	-327 ± 4	-193.4 ± 1.5	-58.2 ± 0.4	37.07 ± 0.14
0.05	74.5 ± 1.4	75.8 ± 0.6	68.44 ± 0.14	43.09 ± 0.04
0.10	39.6 ± 0.8	40.85 ± 0.3	35.2 ± 0.16	20.79 ± 0.04
0.15	18.5 ± 0.5	18.47 ± 0.27	15.9 ± 0.06	9.353 ± 0.015
0.20	7.46 ± 0.3	6.45 ± 0.5	5.98 ± 0.05	3.57 ± 0.011
$B_{V, T_F}^{\text{EM}}(y_{cut})$				
0.01	-453.4 ± 0.14	-391.2 ± 0.13	-276.1 ± 0.12	-157 ± 0.07
0.05	-106.9 ± 0.04	-98.04 ± 0.05	-70.61 ± 0.03	-36.9 ± 0.015
0.10	-40.71 ± 0.025	-37.79 ± 0.03	-27.29 ± 0.018	-12.24 ± 0.01
0.15	-18.25 ± 0.02	-16.7 ± 0.022	-11.99 ± 0.015	-4.578 ± 0.006
0.20	-7.97 ± 0.01	-7.125 ± 0.013	-4.687 ± 0.01	-1.53 ± 0.005
$B_{A, C_A}^{\text{EM}}(y_{cut})$				
0.01	1339 ± 1.7	1072 ± 0.9	629.5 ± 0.3	250.8 ± 0.14
0.05	332.8 ± 0.5	277.2 ± 0.35	163.4 ± 0.17	58.88 ± 0.07
0.10	126.3 ± 0.3	107.1 ± 0.26	61.04 ± 0.16	17.97 ± 0.03
0.15	54.2 ± 0.2	46.08 ± 0.2	25.54 ± 0.1	5.185 ± 0.02
0.20	21.97 ± 0.2	17.9 ± 0.25	9.23 ± 0.08	1.013 ± 0.014
$B_{A, C_F}^{\text{EM}}(y_{cut})$				
0.01	-326.5 ± 4	-164.4 ± 1.2	-15.6 ± 0.3	43.13 ± 0.07
0.05	74.6 ± 1.4	78.6 ± 0.5	66.16 ± 0.13	33.78 ± 0.022
0.10	39.5 ± 0.8	40.8 ± 0.6	34.34 ± 0.08	17.18 ± 0.013
0.15	18.4 ± 0.5	18.7 ± 0.2	15.7 ± 0.07	8.532 ± 0.012
0.20	7.36 ± 0.35	7.29 ± 0.14	5.96 ± 0.05	3.529 ± 0.007
$B_{A, T_F}^{\text{EM}}(y_{cut})$				
0.01	-453.1 ± 0.14	-370.7 ± 0.13	-219.1 ± 0.1	-88.5 ± 0.04
0.05	-106.8 ± 0.04	-93.35 ± 0.04	-57.47 ± 0.023	-22.27 ± 0.009
0.10	-40.69 ± 0.024	-36.04 ± 0.03	-22.83 ± 0.016	-8.066 ± 0.006
0.15	-18.23 ± 0.017	-15.98 ± 0.02	-10.21 ± 0.01	-3.347 ± 0.004
0.20	-7.965 ± 0.01	-6.83 ± 0.013	-4.033 ± 0.008	-1.247 ± 0.0035

Table 7: The EM clustering algorithm.

y_{cut}	$m/E = 0.01$	$m/E = 0.1$	$m/E = 0.2$	$m/E = 0.3$
$B_{V, C_A}^{\text{JADE}}(y_{cut})$				
0.01	1352 ± 2	1088 ± 1.6	727.2 ± 0.5	389.2 ± 0.26
0.05	328.6 ± 0.6	275 ± 0.5	180 ± 0.2	82.34 ± 0.09
0.10	124.2 ± 0.3	106 ± 0.26	66.06 ± 0.15	24.91 ± 0.05
0.15	54.1 ± 0.3	46.84 ± 0.26	28.77 ± 0.1	8.675 ± 0.03
0.20	22.86 ± 0.2	19.84 ± 0.14	12.34 ± 0.09	2.98 ± 0.03
$B_{V, C_F}^{\text{JADE}}(y_{cut})$				
0.01	-787 ± 5	-423.2 ± 1.5	-112.4 ± 0.4	24.27 ± 0.14
0.05	11.7 ± 1.4	25.2 ± 0.7	35.2 ± 0.4	29.65 ± 0.04
0.10	27.8 ± 0.8	29.25 ± 0.33	25.1 ± 0.09	15.33 ± 0.027
0.15	17.45 ± 0.5	16.64 ± 0.24	13.61 ± 0.08	7.885 ± 0.018
0.20	8.7 ± 0.3	7.7 ± 0.14	6.6 ± 0.06	3.796 ± 0.012
$B_{V, T_F}^{\text{JADE}}(y_{cut})$				
0.01	-470 ± 0.16	-380.9 ± 0.16	-255.8 ± 0.11	-138.5 ± 0.06
0.05	-110.8 ± 0.05	-96.21 ± 0.05	-65.03 ± 0.03	-32.06 ± 0.015
0.10	-41.68 ± 0.025	-37.65 ± 0.03	-25.47 ± 0.02	-11.21 ± 0.01
0.15	-18.34 ± 0.017	-16.84 ± 0.025	-11.73 ± 0.013	-4.688 ± 0.007
0.20	-7.834 ± 0.01	-7.252 ± 0.013	-5.176 ± 0.01	-1.955 ± 0.005
$B_{A, C_A}^{\text{JADE}}(y_{cut})$				
0.01	1350 ± 2	1027 ± 1	569.9 ± 0.5	214.1 ± 0.3
0.05	328.6 ± 0.6	261.9 ± 0.4	144.4 ± 0.17	47.69 ± 0.05
0.10	124.1 ± 0.3	101.6 ± 0.3	54.78 ± 0.1	15.35 ± 0.03
0.15	54.15 ± 0.27	45.25 ± 0.2	24.22 ± 0.09	5.72 ± 0.02
0.20	23 ± 0.2	19.12 ± 0.16	10.4 ± 0.12	2.113 ± 0.02
$B_{A, C_F}^{\text{JADE}}(y_{cut})$				
0.01	-785 ± 5	-384 ± 1.8	-59.6 ± 0.3	33.72 ± 0.1
0.05	11.7 ± 1.4	30.6 ± 0.5	38.6 ± 0.2	24.55 ± 0.04
0.10	27.9 ± 0.8	30 ± 0.36	25.05 ± 0.11	12.84 ± 0.02
0.15	17.3 ± 0.5	17.35 ± 0.23	13.73 ± 0.06	6.91 ± 0.01
0.20	8.7 ± 0.3	8.05 ± 0.17	6.66 ± 0.045	3.461 ± 0.01
$B_{A, T_F}^{\text{JADE}}(y_{cut})$				
0.01	-469.7 ± 0.16	-360.5 ± 0.2	-202.8 ± 0.09	-78.07 ± 0.036
0.05	-110.8 ± 0.05	-91.5 ± 0.045	-52.62 ± 0.03	-19.17 ± 0.009
0.10	-41.66 ± 0.025	-35.93 ± 0.03	-21.09 ± 0.015	-7.253 ± 0.006
0.15	-18.33 ± 0.017	-16.1 ± 0.02	-9.935 ± 0.01	-3.29 ± 0.004
0.20	-7.826 ± 0.01	-6.96 ± 0.014	-4.448 ± 0.008	-1.476 ± 0.0035

Table 8: The JADE clustering algorithm.

y_{cut}	$m/E = 0.01$	$m/E = 0.1$	$m/E = 0.2$	$m/E = 0.3$
$B_{V, C_A}^{\text{DUR}}(y_{cut})$				
0.01	443 ± 1.6	329.9 ± 0.5	181.6 ± 0.2	71.09 ± 0.07
0.05	116 ± 0.3	97.26 ± 0.22	52.4 ± 0.12	12.98 ± 0.05
0.10	45.25 ± 0.2	39.53 ± 0.2	22.5 ± 0.09	3.62 ± 0.03
0.15	20.4 ± 0.18	17.82 ± 0.13	10.37 ± 0.08	1.16 ± 0.026
0.20	8.7 ± 0.12	7.61 ± 0.1	4.63 ± 0.05	0.41 ± 0.02
$B_{V, C_F}^{\text{DUR}}(y_{cut})$				
0.01	-128.3 ± 2	-51.2 ± 0.6	10.43 ± 0.18	23.01 ± 0.04
0.05	3.8 ± 1	11.9 ± 0.4	16.8 ± 0.1	10.58 ± 0.024
0.10	6.1 ± 0.5	8.84 ± 0.2	9.98 ± 0.08	5.444 ± 0.017
0.15	4 ± 0.3	4.6 ± 0.15	5.32 ± 0.05	2.824 ± 0.01
0.20	1.44 ± 0.24	2.09 ± 0.1	2.44 ± 0.03	1.039 ± 0.009
$B_{V, T_F}^{\text{DUR}}(y_{cut})$				
0.01	-162.5 ± 0.07	-127.3 ± 0.06	-73.77 ± 0.03	-31.63 ± 0.014
0.05	-42.66 ± 0.026	-37.61 ± 0.034	-23.03 ± 0.02	-7.768 ± 0.008
0.10	-17.37 ± 0.015	-15.8 ± 0.02	-10.49 ± 0.014	-2.996 ± 0.006
0.15	-8.024 ± 0.011	-7.353 ± 0.014	-5.046 ± 0.01	-1.302 ± 0.005
0.20	-3.503 ± 0.008	-3.23 ± 0.01	-2.206 ± 0.008	-0.427 ± 0.004
$B_{A, C_A}^{\text{DUR}}(y_{cut})$				
0.01	443.6 ± 1	313 ± 0.6	146.1 ± 0.17	41.43 ± 0.06
0.05	115.4 ± 0.6	93 ± 0.3	43.97 ± 0.12	8.37 ± 0.024
0.10	45.07 ± 0.22	37.75 ± 0.18	19.15 ± 0.1	2.554 ± 0.02
0.15	20.48 ± 0.16	17.2 ± 0.14	9.11 ± 0.06	0.887 ± 0.016
0.20	8.77 ± 0.12	7.3 ± 0.1	4.04 ± 0.05	0.34 ± 0.018
$B_{A, C_F}^{\text{DUR}}(y_{cut})$				
0.01	-127 ± 2	-42.3 ± 0.7	20 ± 0.16	21.21 ± 0.03
0.05	3.9 ± 0.9	14.5 ± 0.35	18.2 ± 0.1	9.74 ± 0.017
0.10	6 ± 0.5	9.77 ± 0.2	10.44 ± 0.07	5.213 ± 0.011
0.15	4.04 ± 0.3	4.84 ± 0.2	5.51 ± 0.06	2.768 ± 0.007
0.20	1.47 ± 0.25	2.23 ± 0.1	2.5 ± 0.036	1.012 ± 0.006
$B_{A, T_F}^{\text{DUR}}(y_{cut})$				
0.01	-162.4 ± 0.06	-121.3 ± 0.05	-60.29 ± 0.025	-19.36 ± 0.009
0.05	-42.65 ± 0.026	-36 ± 0.03	-19.5 ± 0.016	-5.433 ± 0.005
0.10	-17.36 ± 0.015	-15.15 ± 0.02	-9.073 ± 0.014	-2.345 ± 0.004
0.15	-8.026 ± 0.012	-7.06 ± 0.013	-4.407 ± 0.009	-1.097 ± 0.0034
0.20	-3.499 ± 0.008	-3.093 ± 0.008	-1.934 ± 0.006	-0.369 ± 0.0025

Table 9: The DURHAM clustering algorithm.

References

- [1] R.K. Ellis, D.A. Ross and A.E. Terrano, *Nucl. Phys.* **B178** (1981) 421.
- [2] J.A.M. Vermaseren, K.J.F. Gaemers and S.J. Oldham, *Nucl. Phys.* **B187** (1981) 301.
- [3] K. Fabricius, G. Kramer, G. Schierholz and I. Schmitt, *Z. Phys.* **C11** (1981) 315.
- [4] P. Nason and C. Oleari, *Phys. Lett.* **B387** (1996) 623, [hep-ph/9607347](#).
- [5] P. Nason and C. Oleari, *Phys. Lett.* **B407** (1997) 57, [hep-ph/9705295](#).
- [6] G. Rodrigo, *Nucl. Phys. Proc. Suppl.* **54A** (1997) 60, [hep-ph/9609213](#);
G. Rodrigo, Ph. D. Thesis, Univ. of València, 1996, [hep-ph/9703359](#);
G. Rodrigo, A. Santamaria and M. Bilenkii, *Phys. Rev. Lett.* **79** (1997) 193,
[hep-ph/9703358](#).
- [7] W. Bernreuther, A. Brandenburg and P. Uwer, *Phys. Rev. Lett.* **79** (1997) 189,
[hep-ph/9703305](#).
- [8] A. Brandenburg and P. Uwer, preprint PITHA-97-29, [hep-ph/9708350](#).
- [9] Z. Kunszt and P. Nason, “QCD”, in “Z Physics at LEP 1”, eds. G. Altarelli,
R. Kleiss and C. Verzegnassi (Report CERN 89-08, Geneva, 1989).
- [10] A. Ballestrero, E. Maina and S. Moretti, *Phys. Lett.* **B294** (1992) 425; *Nucl. Phys.* **B415** (1994) 265.
- [11] L. Magnea and E. Maina, *Phys. Lett.* **B385** (1996) 395, [hep-ph/9604385](#).
- [12] K.G. Chetyrkin, R. Harlander, J.H. Kühn and M. Steinhauser, preprint MPI-PHT-97-012, [hep-ph/9704222](#).
- [13] K. Hagiwara, T. Kuruma and Y. Yamada, *Nucl. Phys.* **B358** (1991) 80.
- [14] J. Collins, F. Wilczek and A. Zee, *Phys. Rev.* **D18** (1978) 242.
- [15] P. Nason, S. Dawson and R. K. Ellis, *Nucl. Phys.* **B327** (1989) 49.
- [16] P. Nason and C. Oleari, preprint CERN-TH/97-209, [hep-ph/9709358](#).

[17] P. Nason and B.W. Webber, “QCD”, in “Physics at LEP2”, eds. G. Altarelli, T. Sjöstrand and F. Zwirner (Report CERN96-01, Geneva 1996).